

A miniaturized bioelectronic sensing system featuring portable microbial reactors for environmental deployment

Alyssa Zhou



Electrical Engineering and Computer Sciences
University of California at Berkeley

Technical Report No. UCB/EECS-2017-42

<http://www2.eecs.berkeley.edu/Pubs/TechRpts/2017/EECS-2017-42.html>

May 10, 2017

Copyright © 2017, by the author(s).
All rights reserved.

Permission to make digital or hard copies of all or part of this work for personal or classroom use is granted without fee provided that copies are not made or distributed for profit or commercial advantage and that copies bear this notice and the full citation on the first page. To copy otherwise, to republish, to post on servers or to redistribute to lists, requires prior specific permission.

A miniaturized bioelectronic sensing system
featuring portable microbial reactors
for environmental deployment

by

Alyssa Yuan Zhou

A report submitted in partial satisfaction
of the requirements for the degree of

Masters of Science

in

Electrical Engineering and Computer Science
University of California, Berkeley

Committee:

Professor Michel Maharbiz, Chair

Dr. Caroline Ajo-Franklin

Spring 2017

**A miniaturized bioelectronic sensing system featuring portable microbial
reactors for environmental deployment**

by Alyssa Yuan Zhou

Research Project

Submitted to the Department of Electrical Engineering and Computer Science, University of California at Berkeley, in partial satisfaction of the requirements for the degree of **Master of Science, Plan II**

Approval for the Report:

Committee:



Michel Maharbiz
Research Adviser

10 May 2017

Date



Caroline Ajo-Franklin
Second Reader

10 May 2017

Date

Acknowledgments

First and foremost, I would like to thank my adviser, Dr. Michel Maharbiz and co-adviser, Dr. Caroline Ajo-Franklin for their guidance, support, and encouragement both inside and outside of the lab. They have both created enjoyable and productive work environments without which this work would not have come to fruition.

I would also like to thank Dr. Moshe Baruch, (soon to be Dr.) Tom Zajdel, and Dr. Michaela TerAvest for helping to frame this project and for contributing in numerous ways throughout the life of this project. Dr. Moshe Baruch, in particular, toiled endless hours with me when fabricating the reactors. In addition, Dr. Behzad Rad and Dr. Francesca Manea imparted knowledge on various imaging techniques critical to the characterization of our device.

Finally, I would like to thank my family for their support and love through this journey.

Abstract

Current technologies are lacking in the area of deployable, *in situ* monitoring of complex chemicals in environmental applications. Microorganisms metabolize various chemical compounds and can be engineered to be analyte-specific, making them naturally suited for robust chemical sensing. However, current electrochemical microbial biosensors use large and expensive electrochemistry equipment not suitable for on-site, real-time environmental analysis. Here we demonstrate a miniaturized, autonomous bioelectronic sensing system (BESSY) suitable for deployment in instantaneous and continuous sensing applications. We developed a 2x2 cm² footprint, low power, two-channel, three-electrode electrochemical potentiostat which wirelessly transmits data for on-site microbial sensing. Furthermore, we designed a new way of fabricating self-contained, submersible, miniaturized reactors (m-reactors) to encapsulate the bacteria, working, and counter electrodes. We have validated the BESSY's ability to specifically detect a chemical amongst environmental perturbations using differential current measurements. This work paves the way for *in situ* microbial sensing outside of a controlled laboratory environment.

Contents

| | | |
|----------|--|-----------|
| 1 | Introduction | 3 |
| 1.1 | Microbial Exoelectrogens | 4 |
| 1.2 | Amperometric Biosensors | 6 |
| 1.3 | Thesis Organization | 7 |
| 2 | BESSY Design and Construction | 8 |
| 2.1 | Design of miniaturized potentiostat | 8 |
| 2.2 | Bacterial sensing strains | 9 |
| 2.3 | Design of miniaturized reactors (m-reactor) | 10 |
| 2.4 | Integrating abiotic and biotic structures | 11 |
| 3 | BESSY characterization methods | 13 |
| 3.1 | Confocal fluorescent microscopy | 13 |
| 3.2 | Live/Dead analysis | 14 |
| 3.3 | Colony Forming Unit test | 14 |
| 3.4 | Scanning electron microscopy | 14 |
| 3.5 | Electrochemical system testing | 15 |
| 4 | M-reactor functionality | 16 |
| 4.1 | Viable exoelectrogens are distributed at electron transfer permissible distances | 16 |
| 4.2 | Silica layer acts as filter | 17 |
| 5 | BESSY performance | 20 |
| 5.1 | Detection of sugars | 20 |
| 5.2 | Extraneous cells can be observed | 21 |
| 5.3 | BESSY can independently monitor two m-reactors | 22 |
| 5.4 | BESSY can detect a chemical signal amongst environmental perturbations | 23 |

| | |
|---|-----------|
| 6 Conclusion | 28 |
| 7 Bibliography | 30 |
| Appendices | 36 |
| A Version 1 of BESSY | 37 |
| B A step-by-step guide to constructing an m-reactor | 39 |
| B.1 Preparation | 39 |
| B.2 Construction | 40 |
| B.3 After-care | 43 |
| C Potentiostat Code | 44 |
| C.1 MSP430 C Code | 44 |
| C.2 RedBear Labs Energia Code | 49 |
| C.3 Matlab Code for Extracting Steady State Current | 55 |

Introduction

The ability to sense compounds in aquatic environments is indispensable to monitoring water quality, global climate change, chemical or biological threats, and underwater biodiversity [1, 2, 3]. Traditionally, maritime analysis relied on the manual collection of samples and subsequent analysis on board or after returning to the laboratory [4]. These labor and time intensive processes make it difficult to track trends and offer poor temporal and spatial resolution. To address these challenges, *in situ* chemical sensing techniques have been developed, such as electrical probes, optical spectroscopy, and underwater mass spectrometry [5, 6]. Although versatile, sensitive, and capable of *in situ* deployment, technologies such as the underwater mass spectrometer are still relatively power-hungry, large, and require vacuum systems which may disturb the target environment. Even more limiting is the underwater mass spectrometer's inability to sense non-volatile compounds [1]. Thus, there still exists the need to develop technologies that provide autonomous, deployable, *in situ* monitoring of complex chemicals in aquatic environments.

Since biological systems rapidly detect and report small concentrations of complex chemicals in underwater environments, biosensors are of great interest for *in situ* analysis [2]. The most common type of biosensor utilizes isolated enzymes and antibodies for detection, but these are more suitable for diagnostics, i.e. in-lab detection, as they are only stable in specific conditions, expensive, and susceptible to biofouling [7]. In contrast, microbes are more adept for handling *in situ* environmental sensing by operating across a wide range of pH and temperatures, and having long lifetimes; moreover, they are potentially lower cost [8, 9, 10]. Of particular interest for underwater sensing are microbes that produce electrical current, so-called exoelectrogens [11, 12]. The electronic signal exoelectrogens produce can be detected with low-power, small footprint devices, unlike optical sensors [13]. A network of these deployable biosensors will also offer better temporal and spatial resolution when

monitoring aquatic conditions [4, 14, 15].

1.1 Microbial Exoelectrogens

Exoelectrogens can be used to transduce sensing events into electrical signals through two strategies. First, since exoelectrogens need an electron source to produce current, the native microbes can be used to sense a limited number of sugars that serve as electron donors [16]. Second, chemicals can be selectively sensed by engineering the exoelectrogen. In this latter approach, addition of a small molecule triggers the synthesis of an electron transport protein essential for current production [17]. Since protein synthesis can be regulated by many small molecules, exoelectrogens should be able to sense various analytes.

Shewanella oneidensis MR-1 belongs to the class of exoelectrogens with the capability to transfer electrons from its metabolic pathways to extracellular minerals. The Mtr pathway of *S. oneidensis* contains CymA, an inner membrane tetraheme cytochrome, and MtrCAB, a heterotrimeric outer membrane complex that mediates the direct electron transfer (Fig. 1). This pathway allows the cell to respire by exchanging electrons with solid minerals [19]. In this process of metal reduction, the cells produce measurable electrochemical currents. A number of efforts have centered on incorporating these microbes into electrochemical cells for applications in electrosynthesis, power generation, and biosensing [20, 21, 22].

The correlation between current generation and changes in metabolic activity due to environmental conditions allows these hybrid cellular-synthetic systems to be used as sensors [23]. Many toxic components, including formaldehyde, benzene, and heavy metals, can inhibit metabolic activity, decreasing current production; in contrast, other compounds (often electron donors and carbon sources such as pyruvate) can enhance metabolic activity. By engineering the production of proteins crucial to the Mtr pathway of *S. oneidensis* to be molecule dependent, recent studies have shown the exoelectrogen can detect arsenic [24] and the small molecule arabinose [25]. Using similar methods, many strains of exoelectrogens could be made sensitive to multiple analytes.

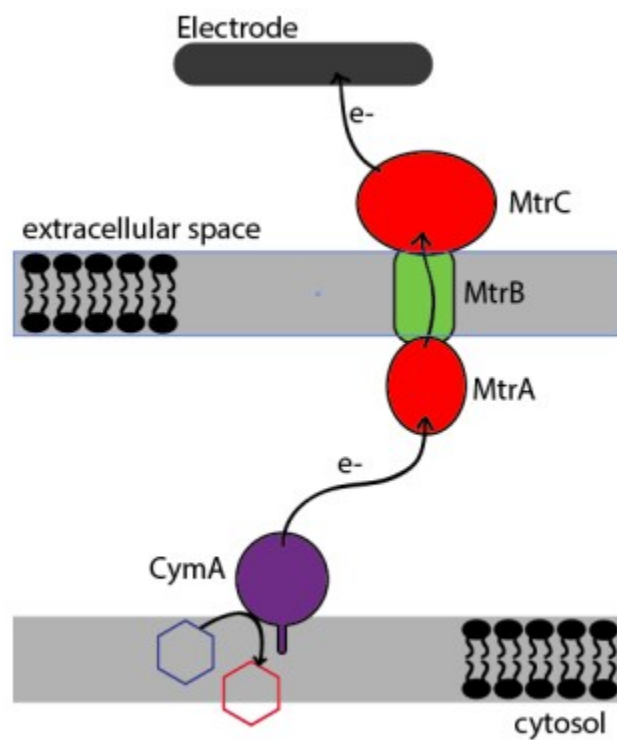


Figure 1: **Mtr pathway of *S. oneidensis*** The electron transport chain consists of CymA, which transfers electrons from the quinol pool to MtrCAB, which allows for the transfer of electrons to a solid metal electrode poised at an anodic potential. Reprinted with permission from "A miniaturized monitoring system for electrochemical biosensing using *Shewanella oneidensis* in environmental applications" by Zhou et al., ©2015 IEEE [18]

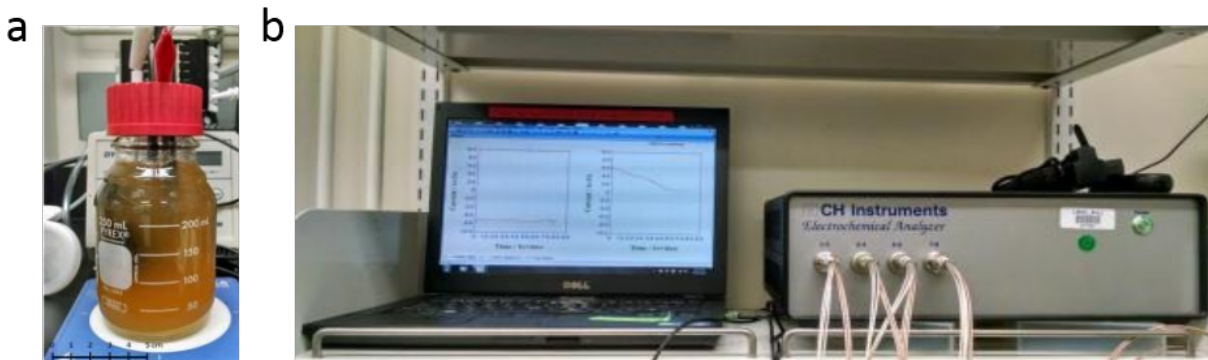


Figure 2: **Traditional microbial electrochemical equipment**(a) A common bioreactor setup to measure metabolic rate through recording current at an electrode. These reactors are large 250 mL jars where sensing bacteria are suspended throughout the whole container. (b) A typical monitoring system for electrochemical analysis. The instruments are large, heavy, power-hungry, and often require physical connection to a computer for live monitoring. This makes mobile, on-site sensing difficult. Reprinted with permission from "A miniaturized monitoring system for electrochemical biosensing using *Shewanella oneidensis* in environmental applications" by Zhou et al., ©2015 IEEE[18]

1.2 Amperometric Biosensors

The sophisticated biological engineering used in these approaches has yet to be matched by the electronics which perform the amperometry and the packaging of the microbes into electrochemical reactors. Conventional monitoring systems for microbial fuel cellbased biosensors require bulky instruments (usually including a potentiostat), as well as off-site lab analysis of samples. This protocol is timely, costly, and hard to implement on-site in real-time (Fig. 2). While there have been recent efforts towards a cost-effective, field-ready potentiostat [26, 5], these briefcase-sized devices leave room for further footprint, power, and cost reduction. Additionally, previous prototypes of miniaturized systems still featured large and cumbersome microbe housing, with the system incapable of distinguishing environmental perturbations (pH, temperature, etc.) from presence of a chemical [27, 28, 18]. We work towards a sensing platform that leverages the advantages of whole-cell biosensors and state-of-the-art electronics technology to create a deployable, low-power sensor for detection in aquatic environments.

1.3 Thesis Organization

In this thesis, we present a novel, miniaturized bioelectrochemical reactor design (m-reactor) which enables engineered bacteria to sample liquid mediums without contaminating the environment. By differentially comparing current production of two strains of electroactive bacteria, a bioelectronic sensing system (BESSY) can uniquely detect chemicals amongst other environmental perturbations.

Chapter 2 begins with the design of the electronics which miniaturizes the previously bulky, expensive, and power hungry amperometry equipment, and offers a wireless means of communication. This chapter then defines the strains of bacteria used in this study, and describes the construction of the miniaturized reactor (m-reactor). The chapter ends with the integration of the abiotic and biotic components to create the deployable BESSY.

Chapter 3 describes the methodology used to characterize the BESSY, including confocal fluorescent and scanning electron microscopy techniques, Live/Dead and CFU testing, and electrochemical analysis.

Chapter 4 summarizes the results of the M-reactor characterization and functionality.

Chapter 5 details the performance of the BESSY and the sensing results when placed in various environments. Specifically, we demonstrate

1. the ability of native *S. oneidensis* to sense the presence of pyruvate through increased metabolic reaction rates
2. the ability to infer presence of other microbes in the environment
3. the ability to independently monitor two m-reactors
4. engineered exoelectrogen's ability to detect a target analyte amongst environmental perturbations

The microbial based BESSY developed in this thesis contribute to the ultimate vision of producing a cm-scale untethered, autonomous recording “mote” which includes an encapsulated, healthy population of electroactive bacteria (e.g. *S. oneidensis*) capable of *in situ* reporting of analyte concentrations via electrodes using electron-transfer pathways.

The conclusion in Chapter 6 suggests future work towards this goal.

BESSY Design and Construction

The first step in creating a mobile electrochemical sensing platform was miniaturization of the monitoring electronics. One common method to measure the current signals produced by the electron transfer from *S. oneidensis* is using a potentiostat. This method uses a three electrode set-up that controls a voltage potential between a working electrode (WE) and a reference electrode (RE), and measures the resulting current between the working and counter electrode (CE) [29]. Departing from traditional glass reactors to a miniaturized, mobile microbial reactor is also necessary in designing a deployable sensor. This structure must keep cells viable and contained, while also allowing chemical movement with the outside environment and providing a semi-solid matrix where cells are held at a favorable distance from the electrode. The final BESSY must incorporate both abiotic and biotic components in a way that shields the electronics from aqueous, corrosive elements, but exposes the microbes to target environmental analytes. A floating, passive sensor which can randomly sample various regions of a body of water would also be beneficial in obtaining a more comprehensive view of its chemical composition. In this chapter, the final version of the BESSY is described. Previous versions of the device are discussed in the appendix.

2.1 Design of miniaturized potentiostat

Our custom potentiostat chip is assembled with all commercially available components including (1) a MSP430FG437 low power microcontroller featuring an integrated digital to analog converter (DAC), analog to digital converter (ADC), and three on chip programmable operational amplifiers (op amp), (2) capacitors and resistors for biasing, (3) a 32 kHz crystal for timing, (4) a TS5A23159 analog switch, and (5) input/output ports for connecting to working, counter, and reference electrodes as well as a power supply. The DAC was used to

output a 200 mV potential which was summed with the Ag/AgCl RE so that the potential of the WE was 200 mV above the reference. The three op amps each perform a separate task, including (1) buffering the RE potential, (2) driving the WE potential, and (3) amplifying the current signal before recording at the ADC. The potentiostat is configured such that only one channel is operational at a time and alternates between both channels (Fig. 1a,b), thus avoiding crosstalk between the two channels induced by current collection on the same RE. Although the frequency of switching can be adjusted, for this study the system measures each channel for ten minutes at a time. This time is approximately how long it takes for the measured current to settle to steady state after each switch (measurements are taken at fifteen second intervals). This switching of channels allows for two independent electrochemical measurements to be taken with the machinery of only one channel, reducing power and footprint. Moreover, this switching allows a single device to sense the target analyte in the environment in the presence of other variables by taking differential measurements between a responsive and a null strain. The MSP430 microcontroller then outputs this data through serial ports to the RedBear Lab’s WiFi Micro for small footprint wireless communication capabilities. Together, the platform consumes 30 mW when sampling and transmitting information once every 15 seconds, with the majority of the power going to WiFi communications. For even lower power consumption, the data could also be stored locally on a SD card. Figure 3a and b illustrate the circuit and its final 2x2 cm² size. The MSP430 and WiFi Microchip were programmed using Code Composer Studio and Energia, respectively.

2.2 Bacterial sensing strains

Four strains of the exoelectrogen, *Shewanella oneidensis*, were used to validate our platform’s sensing capabilities: (1) wild type *S. oneidensis* MR-1 [30], (2) a mutant of *S. oneidensis* unable to produce current, Δ mtrB [31], (3) a mutant of *S. oneidensis* unable to reduce fumarate, Δ fccA [32], and (4) a GFP-expressing strain of *S. oneidensis* containing the p519nGFP plasmid [33]. Cultures were inoculated from frozen glycerol stocks into 250 mL erlenmeyer flasks containing 50 mL 2xYT medium and grown overnight at 30°C with 250 rpm shaking. Fifty μ g/mL kanamycin was added to the growth medium for both Δ fccA and GFP-expressing *S. oneidensis*. After overnight growth, the cells were harvested by centrifugation.

gation at 5000g in 4°C for 10 minutes and washed twice with M9 medium. Finally, cells were prepared for injection into the m-reactor by resuspension of the cell pellet in M9 medium until the cell density corresponded to an OD_{600nm} of ~120 (typically 300-400 μL M9 medium added). This cell suspension was kept on ice until used for reactor construction.

2.3 Design of miniaturized reactors (m-reactor)

To avoid contamination of the m-reactor with non-exoelectrogenic bacteria, it is important for all the abiotic components of the assembly to be sterile and for the construction to occur in a sterile environment. To create the working electrode compartment, conductive carbon felt was shredded to a fine powder and UV sterilized. Next, 250 mg of this carbon felt powder was mixed with 150 μL of the *S. oneidensis* cell suspension (OD_{600nm} ~120) and 1.4 mL of 1% per agarose, heated to 55°C. Then, the carbon felt-bacteria-agarose mixture was compressed into a 2x1x1 cm³ container, which had been coated with 1% agarose, until the mixture was approximately a half-cm in height. To append the counter electrode compartment, a 3D printed polylactic acid (PLA, a biodegradable thermoplastic) scaffold with a titanium wire wrapped around the topmost part was then inserted until it penetrated the compact mixture. This scaffold improved mechanical stability and ensured the counter electrode wire did not short with the working electrode carbon felt. Lastly, 1% agarose was added to the container until it completely covered the titanium wire (~3 mL). After cooling at room temperature ~15 minutes, or until agarose solidified, the assembly was delicately extracted from the container and a second titanium wire was inserted and secured into the carbon felt-bacteria-agarose mixture to become the working electrode connection. To create a filter, the complete assembly was fully dipped and covered in 0.5% agarose before placing in a dessicator with 8 mL of tetramethyl orthosilicate (TMOS) and left for evaporation for ~2 hours. This step deposited thin films of silica onto the assembly for bacterial containment. After removal from the dessicator, the complete m-reactor was placed immediately in M9 medium to prevent drying out. Figure 4 shows the final, constructed m-reactor and provides a cartoon schematic of its components. A more detailed, step-by-step guide to this assembly process with visuals is available in Appendix B.

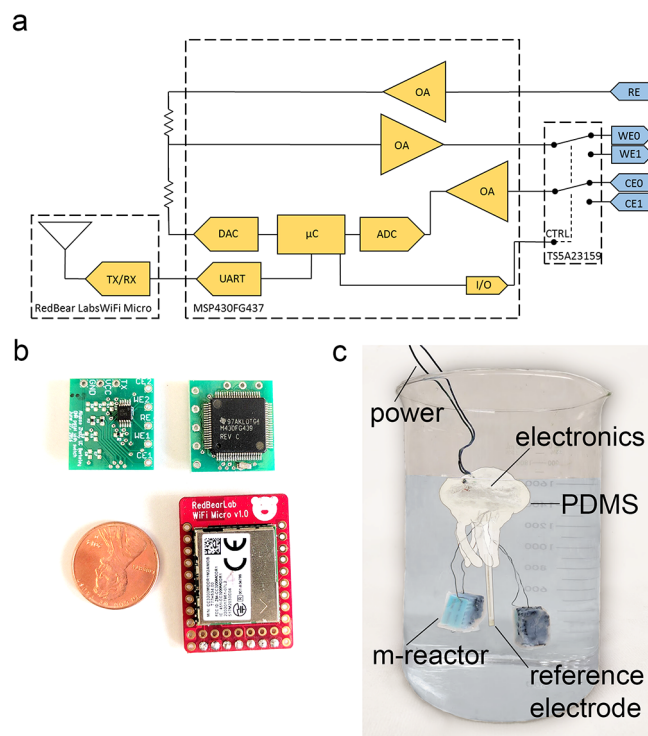


Figure 3: **A miniaturized BESSY for deployable electrochemical monitoring.** (a) Circuit diagram of COTS potentiostat featuring three on chip op amps on a MSP430FG437 microcontroller sending serial data to Redbear Labs Wifi Micro board for wireless data transmission. Only circuitry for one three-electrode channel is on board, but switching results in multiple channel potentiostat function. (b) Final potentiostat PCB (green) footprint is $2 \times 2 \text{ cm}^2$ and is connected to WiFi micro board (red). (c) Contrast corrected photograph of the BESSY for differential sensing and deployment in aqueous environments.

2.4 Integrating abiotic and biotic structures

Casing for electronics was cast with PDMS (Dow Corning, Sylgard[®] 184 Silicone Elastomer Kit) in a mold formed with silicone molding rubber (Smooth-On, OOMOO[®] 300), both mixed according to manufacturers' instructions. The mold was constructed to resemble a jellyfish as inspiration for a sensor that floats around a body of water sampling the various regions and reporting its sensor results. The m-reactors and Ag/AgCl RE were attached and connections to the electronics made by piercing the PDMS with the wires to the electronics cavity and soldering to the connection pads. Silicone rubber (Dow Corning[®] 732

Multi-Purpose Sealant) was used to seal and waterproof the connection sites through the PDMS. Figure 3c displays the final BESSY floating in a beaker of water. This buoyant, biocompatible, waterproof PDMS casing protects the electronics and allows the system to sample environmental conditions of an enclosed body of water.

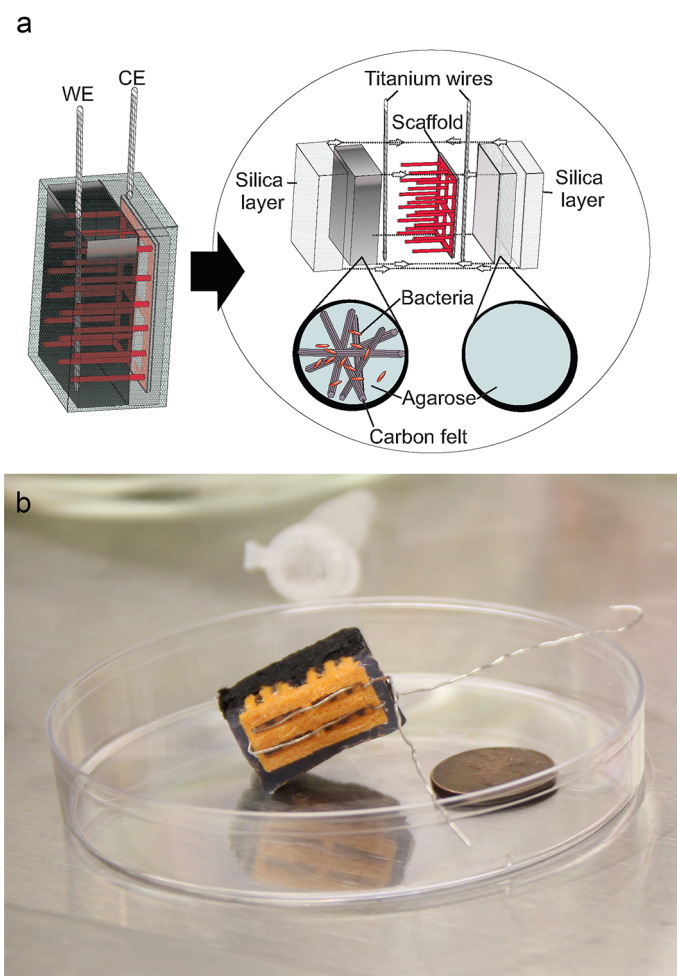


Figure 4: **M-reactor for microbial integration** (a) Conceptual schematic of m-reactor detailing how the scaffold stabilizes the bacteria containing, carbon felt WE compartment (black) with the nonconductive, agarose, CE compartment (gray), and how a silica layer coats the device. (b) Realization of m-reactor.

BESSY characterization methods

In order to characterize and test the performance of the BESSY, we use a number of imaging and electrochemical techniques, as described in the following passages.

3.1 Confocal fluorescent microscopy

To visualize interactions between the exoelectrogenic bacteria and the conductive carbon fiber, fluorescent microscopic images of the m-reactor were taken on a Zeiss LSM710 confocal microscope with an Axio Observer Z1. Samples of the m-reactor were fixed by submerging in 4% formaldehyde for 20 minutes. Afterwards, samples were washed three times with milliQ H₂O, and allowed to sit for 5 minutes in the milliQ H₂O between each wash. Samples were stored in M9 medium in a 4°C refrigerator until they were ready to image. Prior to imaging, samples were stained in 14.3 μ M DAPI (Thermo Fisher) in M9 medium and 1 μ M Cy5 (Thermo Fisher) for 10 minutes at a time. The DAPI stain identifies individual bacteria by their nucleus and the Cy5 provides a nonspecific agarose stain for better carbon felt contrast. Samples were removed from the dye solutions and placed in M9 medium on a glass bottom 6-well plate (Mattek Corporation, P06g-1.5-20-F) and imaged either with a 10x EC Plan-Neofluar objective (0.3 NA) or 100x Plan Apochromat oil immersion objective (1.4 NA). Confocal stacks of the sample were obtained using a 405 nm diode laser to excite DAPI and a 633 nm HeNe laser to excite Cy5, both using a 33.63 μ m wide pinhole. The image shown in Figure 5 was falsely colored to enhance contrast for visualizing the sample.

3.2 Live/Dead analysis

The m-reactor was cut into small samples for live/dead analysis. To create control samples that contained only dead cells, pieces of the assembly were immersed in 70% isopropanol, a disinfectant, for 5 minutes. We used LIVE/DEAD[®] BacLight[™] Bacterial Viability Kit (ThermoFisher Scientific, Product number L13152) following the manufacturer's instructions with slight modifications to accommodate the solid nature of the samples, as follows. One mL of the 5 mL 2X stock solution containing both SYTO 9 dye and propidium iodide was mixed with 1 mL of M9 medium, and then 2 mL of this solution was used to stain the m-reactor. The sample was incubated at room temperature in the dark for 15 minutes and then washed five times with M9 medium before observation. Fluorescent images were acquired on a Zeiss LSM710 confocal microscope with an Axio Observer.Z1 using the 10x EC Plan-Neofluar objective (0.3 NA) with the pinhole set to 33.63 μm . SYTO9 was excited with a 488 nm Argon laser and the emission was monitored between 493-556 nm. Propidium iodide was excited using a 561 nm DPSS laser with the excitation monitored between 593-719 nm. The live (green fluorescent) and dead (red fluorescent) signals were collected and the ratio between the two signals was determined, while maintaining constant light intensity and gain. We used the dead samples as a control for our assembly samples.

3.3 Colony Forming Unit test

Silica-coated and silica-free m-reactors were prepared and placed in 50 mL Falcon tubes containing 40 mL sterile M9 medium. On the indicated time points (t=0, 24, 48, 72 h), samples of the medium were taken, diluted with sterile M9 medium, and spread on solid lysogeny broth (LB) medium containing 1.5% agar. Plates were incubated overnight at 30°C and resulting colonies were counted.

3.4 Scanning electron microscopy

Thin slices of the m-reactor were cut and placed in Tris buffer (pH 7.5). Glutaraldehyde to a final concentration of 2.5% (v/v) was added to the slices and incubated for 20 min to fix the samples. Serial dilutions of ethanol (10, 25, 75, 90, 100% ethanol) were applied at 15

minute increments to dehydrate the sample. The slices were placed in closed petri dishes and left to dry overnight in a fume hood. Specimens were sputtered with gold to an approximate thickness of 10 nm prior to visualization. The field emission scanning electron microscope used was the FESEM Ultra 55 set to an EHT (extra high tension) voltage level of 3-5 kV, under vacuum (5.0×10^{-5} mbar), and working distance of 4-7 mm.

3.5 Electrochemical system testing

Experiments were conducted in 1 L beakers full of M9 medium. The BESSYs were exposed to various environments to test its response in each scenario. Specifically, the environments discussed in this thesis include:

1. wild type *S. oneidensis* in M1 medium with and without 50 mM pyruvate
2. wild type *S. oneidensis* in M1 Medium with 0.4% glucose and addition of *E. coli*
3. wild type and Δ mtrB *S. oneidensis* in M9 medium with addition of 40 mM lactate
4. wild type and Δ fccA *S. oneidensis* in M9 medium with addition of 10 mM lactate followed by 1 mM fumarate
5. wild type and Δ fccA *S. oneidensis* in M9 medium with 10 mM lactate into an ice bath for 8 hours and returned to room temperature at benchtop

Three-electrode potentiostat measurements were taken by setting the potential of the WE of each active reactor at +200 mV with reference to a 3 M Ag/AgCl RE. The custom potentiostat was programmed to collect current readings every 15 seconds. The data was transmitted either to an SD card (Sparkfun, OpenLog) or through RedBear Labs Wifi Micro board to a Google Documents spreadsheet using Temboo, Inc's commercially available WiFi Choreos. In the final, dual-channel potentiostat, the device switched between the two channels every 10 minutes such that only one is active at a time, to prevent any crosstalk between the reactors. In this case, every time a channel was switched on, there was a period of exponential decay when the cells expelled a buildup of charge, which accumulated during the period of inactivity, through the capacitive-like membrane. Therefore, the raw data was fit to an exponential decay curve for each 10 minute set of data and extrapolated the cells steady state current output (Appendix C.3). In both versions of the BESSY, collected data passed through a five-point moving average in post processing to reduce noise.

M-reactor functionality

The m-reactor is designed to collect current from an exoelectrogenic bacterial strain that is sampling the environment. To achieve this, (1) the bacteria must survive the fabrication process and be housed in an environment conducive to cell viability, (2) the bacteria must be within electron transfer distance of a charge collector, and (3) the bacteria must be surrounded by a size-selective filter to prevent their release, yet permit diffusive transport of small molecules. Thus, we designed an assembly in which a 1% agarose gel contains carbon felt fibers and the bacteria, which is electrically connected to a titanium wire to create a WE. This WE is separated by ~ 5 mm from a titanium wire counter electrode which is also embedded in agarose. An evaporated silica layer encases both electrodes. The fabrication process described in Section 2.3 allows for (1) custom geometries through molding, (2) room-temperature, non-desiccated assembly, and (3) a size-selective filter using tetramethyl orthosilicate (TMOS) silica deposition, thus obviating the need for chemical or physical sealing of reactor chambers.

4.1 Viable exoelectrogens are distributed at electron transfer permissible distances

In order to visualize how the bacteria are distributed among the conductive fibers in our m-reactor, we stained the bacteria with DAPI and Cy5 and took fluorescent confocal images of our constructed electrodes. These images (Fig. 5a) suggest that the bacteria are randomly aggregated in tight clusters around the conductive fibers, which allows them to deliver current to the carbon fibers. As seen by their positioning around the carbon felt, a significant number of *S. oneidensis* are within $10 \mu\text{m}$, which should allow for electron

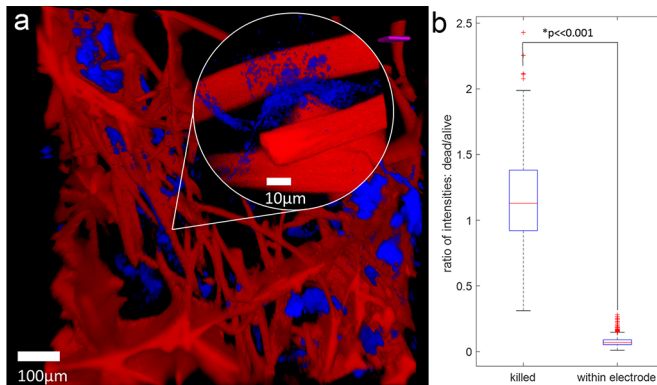


Figure 5: **Microbial viability following m-reactor construction** (a) Fluorescent confocal microscopy image of electrodes to visualize internal interaction of bacteria (blue) with carbon felt (red). Inset shows a closeup of bacteria intertwining the conductive carbon felt, illustrating $<10 \mu\text{m}$ distance between the exoelectrogens and felt. (b) Distribution of the ratio of intensities for control dead cells ($n=173$) and samples of our reactor ($n=685$). The $p < 0.001$ chance of similarity indicates that sampled bacteria are not significantly disturbed.

transfer by all known mechanisms: direct electrode contact, soluble flavin mediators, and contact through conductive nanowires [34, 35].

To determine the survival rate of the bacterial population through this construction process, we performed live/dead assays on the bacteria in the electrode. The bacteria in isopropanol-sterilized control samples had an average fluorescent intensity ratio of 1.6 ($n=173$), which is consistent with these cells being dead. In contrast, the fluorescence intensity ratio in the samples from the m-reactor averaged 0.07 and had no overlap in distribution with the isopropanol control (Fig. 5b), indicating that the sampled cells were not significantly disrupted ($n=685$, $p < 0.001$). This confirms the described m-reactor construction process enables encapsulation of viable microbes.

4.2 Silica layer acts as filter

To probe the ability of the silica layer to act as a size-selective filter, we scored the extent to which the bacteria diffuse out from the m-reactor. We performed CFU tests on the surrounding medium for both silica-coated ($n=3$) and naked, agarose only ($n=3$), m-reactors over a 72 hour time period. Without the silica coating, the bacteria diffuse out through the

agarose and contaminate the environment. In contrast, the electrodes coated with silica did not show contamination of bacteria past $t=0$ h (Fig. 6a). This demonstrates silica's effectiveness in containing the bacteria inside the m-reactor and preventing contamination of the surrounding medium by our genetically modified bacteria. It also implies that the silica will prevent bacteria in the environment from infiltrating our device.

To ensure that this silica filter does not erode over the course of the experiment, we took scanning electron micrographs (SEMs) of our electrode immediately after silica deposition and again after two weeks of experiments (Fig. 6b). These images show robust silica encapsulation with evidence for <200 nm pores and the absence of >2 μm pores. Moreover, the multiple layers of the porous silica surface form tortuous paths, confirming that the silica acts as a filter confining the bacteria, typically 2-3 μm in length and 0.4-0.7 μm in diameter [36]. The consistency of the silica coating at these time points also demonstrates the filter does not visibly disintegrate over the course of the experiment and maintains containment. The current silica deposition process results in a ~ 1 μm thick silica layer. This is adequate for the containment of bacteria for the lifetimes of experiments in this application, but it should be noted that altering evaporation time, temperature, and pressure conditions controls silica thickness and conformality, which can be engineered for containment of bacteria of different sizes. These m-reactors offer a versatile platform for deployment into almost any aquatic environment for analyte sensing.

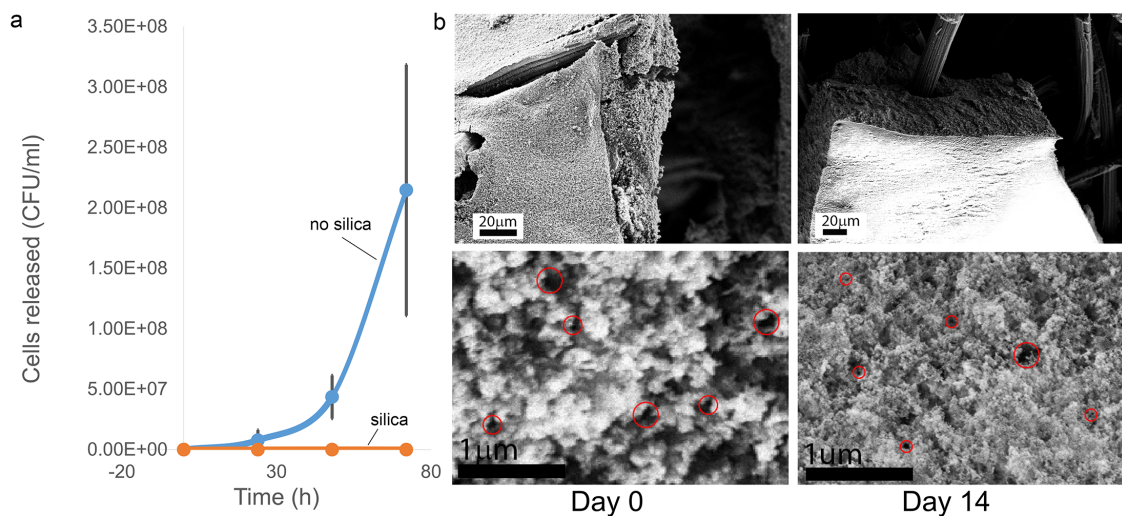


Figure 6: **Silica filter characterization** (a) The effectiveness of silica in containing bacteria is tested by CFU tests with samples taken at $t=0$, 24, 48, and 72 hours. The bare electrode (blue) shows leakage of bacteria through the electrode whereas the silica on the coated electrode (red) acts as a filter, preventing this contamination. (b) Scanning electron micrographs (SEM) of electrode surface showing the silica coating ($1 \mu\text{m}$ thick, 2 hour deposition) and further magnification to determine that pore size is less than $\sim 0.2 \mu\text{m}$ (samples circled in red) taken at $t=0$ and $t=14$ days. Absence of significant visual discrepancies indicates the coating does not degrade over the lifetime of these experiments.

BESSY performance

In this chapter we discuss the BESSY's response to a number of different environmental conditions. The first two sections (5.1 and 5.2) are results from the first version of BESSY (see Appendix A). We expect the same results from the final version of the BESSY because there is no evidence the changes made, specifically binding the microbes in agarose, will affect the electrochemical current production of the exoelectrogens. It should be noted that some of these results are excerpted from a previous publication [18]. This chapter closes by demonstrating how a two-channel potentiostat can detect chemical signals amongst representative environmental fluctuations using differential current sensing.

5.1 Detection of sugars

The proteins in the Mtr pathway of *S. oneidensis* provide the electron conduit necessary to allow the cell to respire on the electrode. This metabolic reduction at the anode produces a current, our sensor's signal of interest. The magnitude of these currents is directly proportional to the rate of bacterial metabolism, which we can control by altering the concentration of substrates present. We target pyruvate as the substrate of interest in this section. Pyruvate donates its electrons to the electron transport chain, resulting in the production of ATP and NADH. Therefore, we can potentially correlate changes in current production from the cells with presence of pyruvate in its environment.

To see the effects of pyruvate as an environmental stimulus of encapsulated *S. oneidensis*, the BESSY was introduced to a pyruvate-free environment, allowed to stabilize, and then placed in a solution of 50 mM pyruvate. This was repeated to demonstrate the current levels rising and falling depending on the substrates the cells have access to. We also measured the optical density of the environmental solution to demonstrate the effectiveness of the

commercial 200 nm membrane and ensure that the *S. oneidensis* remained contained within the package and did not contaminate the external medium.

As the sensor moved from pyruvate-poor to pyruvate-rich environments, the current signal increased in response from 40 μA to 55 μA (Fig. 7). When the cells returned to an environment without pyruvate, the current production fell back down to 20 μA . This change in signal could be the result of two effects of pyruvate. First, the metabolic rate of individual bacterium increased due to the increase in substrate, similar to any chemical reaction in equilibrium. Second, the cells may have been duplicating, resulting in more bacteria available to attach to the electrode and contribute current. Delays in the response to the presence of pyruvate may be due to the finite time required for the chemical to diffuse across the porous membrane, and reach the electrochemical cells. Optical density measurements of the surrounding solution were taken with respect to baseline M1 media and was 0.002 absorbance, significantly lower than the optical density within the package (0.441 absorbance). These experiments were not done in a sterile environment, and random particles may account for the slight increase in absorbance. We can conclude that the membrane effectively contained the *S. oneidensis* from the surrounding environment but still allowed diffusion of chemicals for sensing.

5.2 Extraneous cells can be observed

We assessed the relationship between extraneous organisms and the current production of our exoelectrogenic cells in controlled environments. *S. oneidensis* cannot metabolize glucose; however, *E. coli* can ferment glucose to produce pyruvate, and pyruvate, in turn, can then be oxidized by *S. oneidensis*. We allowed the biosensor to equilibrate in M1 medium with 0.4% glucose and injected *E. coli* to the solution to reveal that *S. oneidensis* can sense the presence of the increase of pyruvate, and by extension, the extraneous *E. coli*. When the *S. oneidensis* was in a solution of glucose, it stabilizes at a relatively low current level of 40 μA . Once the *E. coli* was introduced to the surrounding solution and fermented glucose to produce pyruvate, among other byproducts, the *S. oneidensis* within our sensor started to undergo metabolic respiration and, as a result, current signals increase to 65 μA (Fig. 8). This test showed a longer delay to recognize the presence of *E. coli*, most likely because we are indirectly measuring its presence through a chemical byproduct, in addition to diffusion.

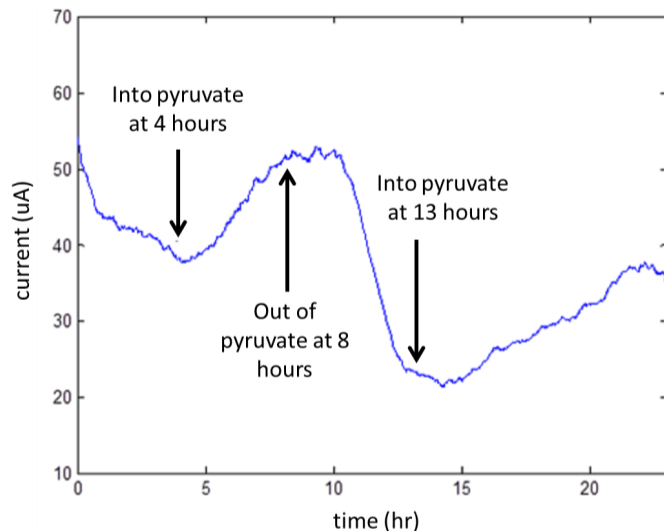


Figure 7: **Pyruvate response** *S. oneidensis* current production as BESSY is transferred from no pyruvate to 50 mM pyruvate environment. Transfer times occurred at $t=4$, 8, and 13 hours.

Although the cells are physically separated by the membrane, *S. oneidensis* can still sense the presence of *E. coli*. Current growth could signal the presence of organisms in the solution capable of metabolizing glucose to pyruvate. In environments where it is known that no active metabolite is present, an increase in current could signify the presence of a foreign microbe.

5.3 BESSY can independently monitor two m-reactors

When moving from a one-channel to two-channel potentiostat for differential current sensing, we validated the BESSY's ability to accurately monitor electrochemical signals from separate m-reactors without cross-talk by measuring the lactate response signals for lactate responsive (wild-type) and lactate null ($\Delta mtrB$) strains of *S. oneidensis*. As expected, reactors populated with the lactate null strain produced low current and did not respond to lactate addition. In contrast, the lactate responsive assembly initially showed a decrease in current from nutrient starvation in minimal M9 medium and then responded to 40 mM lactate injection with a $\sim 19 \mu A$ jump in current (Fig. 9). This demonstrates the BESSY's

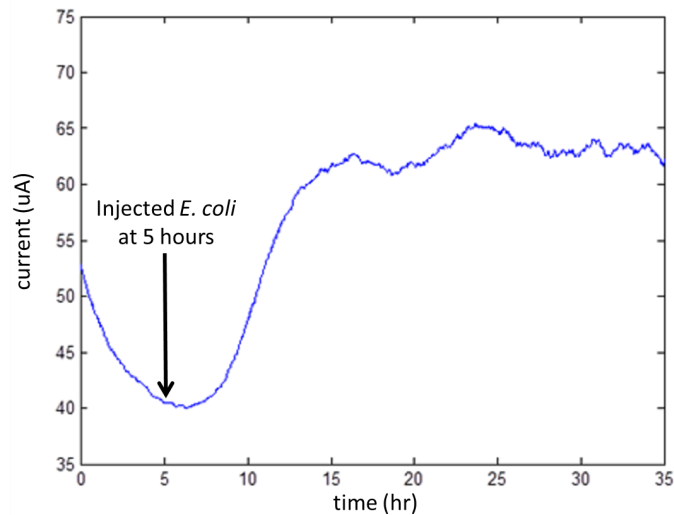


Figure 8: *E. coli*'s effect on the BESSY *S. oneidensis* current production over time as biosensor sits in a glucose rich environment and *E. coli* is introduced to the solution ($t=5$ hours).

ability to perform two-channel, three-electrode electrochemical amperometry with our novel m-reactor design. These data also indicate that (1) the electrogenic bacteria are able to reduce the carbon fibers which remain in conductive contact with the titanium working electrode, (2) small chemicals, in this case lactate, can diffuse into the assembly, and (3) the system can independently record two channels using the switching mechanism. This meets the additional three requirements necessary for a sensing platform.

5.4 BESSY can detect a chemical signal amongst environmental perturbations

The BESSY is designed to monitor electrochemical signals from two bacterial strains with different sensing abilities to filter out chemically-induced responses from environmental variables such as temperature. To determine the BESSY's ability to ignore environmental changes, we created a fumarate sensor employing fumarate null ($\Delta fccA$) and fumarate responsive (wild type) strains of *S. oneidensis* and observed the effects of temperature on this sensor. The fumarate sensor was cooled to 4°C with an ice bath for 8 hours and warmed back

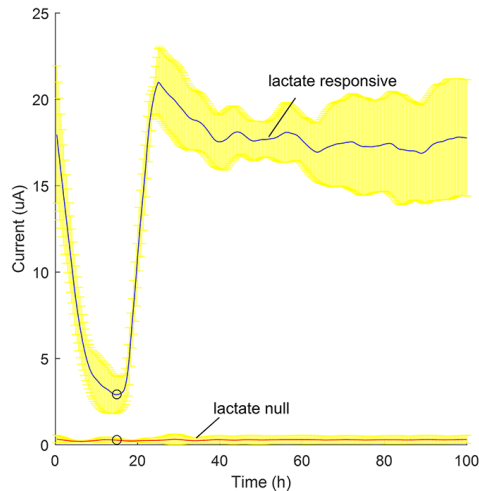


Figure 9: **Two-channel lactate sensing** Average lactate responsive (blue) and lactate null (red) current response to 40 mM lactate injection at $t=16$ h (o), with standard deviations (yellow) for three technical repeats of one of two similar biological repeats. The $\sim 19 \mu A$ increase in current demonstrates the microbes’ ability to proliferate and reduce the carbon fibers while allowing environmental chemicals to diffuse in and out of the silica coated electrode. It also demonstrates sensing of multiple channels using one device without crosstalk.

to room temperature to imitate extreme fluctuations that the sensor could experience in deployment (Fig. 10a). Both strains of *S. oneidensis* showed decreased and increased current production with the fall and rise of temperature, respectively. Indeed, calculating the ratio of the current produced by the analyte responsive strain over the null strain ($I_{\text{responsive}}/I_{\text{null}}$) shows that this ratio did not significantly change upon cooling or heating (Fig. 10b). These controlled experiments indicate environmental fluctuations result in RMS noise of approximately $0.05 I_{\text{responsive}}/I_{\text{null}}$. Any target analyte will have to instigate a response greater than this noise floor in order to be detected.

To test the BESSY’s ability to selectively sense one target analyte amongst other chemicals, we probed the ability of our fumarate sensor to distinguish between fumarate and lactate. When lactate is introduced at $t=20$ h, both strains in the BESSY produce more current (Fig. 10c) and the ratio between the currents does not change significantly (Fig. 10d), which confirms the BESSY’s ability to ignore chemicals of disinterest. The RMS noise of the ratio up until the injection of fumarate continues to be approximately $0.05 I_{\text{responsive}}/I_{\text{null}}$.

Because fumarate is an alternative electron acceptor to the metal electrode [37, 38], we

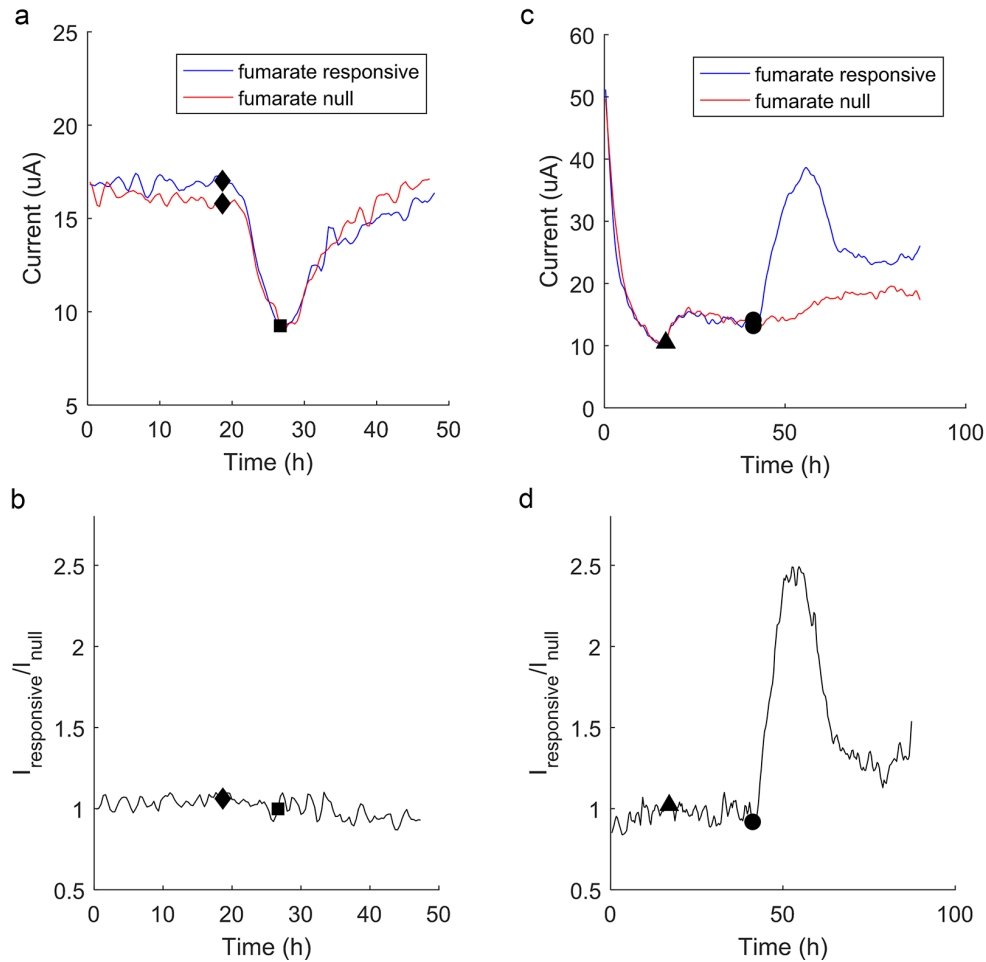


Figure 10: **Fumarate BESSY responds amongst chemical and temperature perturbations** (a) Current in response to temperature fluctuations over time, simulated by immersing in an ice bath (◆) and removal from ice bath (■), shows both strains decrease and increase current production similarly. (b) The ratio of the two strains as a function of time does not change significantly, with RMS noise ~ 0.05 . In this way, the sensor can filter out environmental variables such as temperature when deployed for environmental sensing. (c) Current in response to chemical perturbations over time illustrates an insignificant response when 10 mM lactate is added (▲), and a significant differential response when 1 mM fumarate is added (●). (d) The ratio of the two currents shown above as a function of time. As expected, there is no significant fluctuation in the ratio upon addition of lactate, which contrasts the fumarate response. Figures shown here are representative of two biological repeats, each with three technical repeats. Response time, defined by time to reach two standard deviations above the average environmental noise, is 1.8 ± 0.7 hours, and the maximum ratio of $I_{\text{responsive}}/I_{\text{null}}$ is 2.1 ± 0.4 .

expect to see a decrease in current from the wild type (fumarate responsive) strain since the *fccA* reduces the fumarate directly. Moreover, because fumarate is consumed in this process, we expect only a temporary current response. On the contrary, little response is expected in the $\Delta fccA$ (fumarate null) strain due to its inability to reduce fumarate [39]. As expected, only the fumarate responsive strain changes its current production upon the addition of fumarate. When 1 mM fumarate is injected at $t=45$ h, there is a significant increase in the ratio which decreases, presumably once the fumarate has been consumed, around $t=65$ h. The response time of this system to fumarate, defined by time to reach two standard deviations above the average environmental noise, is 1.8 ± 0.7 hours. At this time, we can be 95% confident that the BESSY has detected fumarate, and the signal is not fluctuating due to a change in temperature or lactate concentration. The maximum ratio of $I_{\text{responsive}}/I_{\text{null}}$ is 2.1 ± 0.4 following the injection of fumarate. Through these experiments, we have proof of concept that differential sensing is a valid method for normalizing microbial biosensing to uncontrollable environmental variables. Moreover, we have demonstrated the functionality of this methodology on a miniaturized platform for deployable sensing.

It is surprising, however, that the wild type *S. oneidensis* always showed a positive change in current upon addition of fumarate in our system. We speculate that this is a result of the switching feature imposed on both channels: because only one working electrode is poised at a favorable potential at a time, the bacteria in the channel which is “off” are without an electron acceptor for ten minutes at a time. Therefore, when the alternate electron acceptor, fumarate, appears in the solution, the fumarate-responsive bacteria can metabolize continuously. We suspect these conditions result in higher overall current production in the fumarate-responsive strain. This reasoning suggests that utilization of some sensing strains within our system may yield in changes in $I_{\text{responsive}}/I_{\text{null}}$ that have the opposite sign as what is observed when performing continuous monitoring. It is important to note that for the application of detection of target chemicals between an analyte sensing and null strain, as is demonstrated here, the direction of change is not as important as a proportional change in current. By setting a threshold for the ratio of $I_{\text{responsive}}/I_{\text{null}}$, for example at ~ 1.5 , the system can alert when the ratio peaks. Depending on the application, this threshold can be set to be very conservative, alerting the user at the slight possibility of signal, or rather liberal in monitoring uses where the chemical is not hazardous. Using the BESSY with an engineered selection of analyte sensitive electrogenic bacteria, we can make our device specific

to only our target analyte and detect fumarate amongst environmental perturbations, such as temperature and variations in other chemicals.

Conclusion

We have demonstrated a miniaturized alternating potentiostat capable of using differential signal measurements to detect various chemicals amongst other environmental variables. We have also designed a small, portable m-reactor to contain exoelectrogenic bacteria without contaminating its surroundings. This 2x1x1 cm³ assembly is more than 10x smaller in volume than other submersible microbial biosensors [40, 41]. Moreover, most of the currently existing *in situ* biosensors focus on mobilizing the reactor assembly but still rely on bulky external electronics, such as a commercial multimeter [42, 43]. They often also require calibration for different environmental conditions such as pH and temperature [41]. By miniaturizing the electronics and incorporating an analyte sensing and null strain, this work introduces the concept of a fully mobile, easily deployable BESSY (bioelectronic sensing system) for environmental sensing. The differential sensing system enables self-calibration in various environments, in the same way that we show for temperature and variability in nutrients (lactate), provided the same type of differential correction could be made for changes in pH, alkalinity, and other conditions. This biosensing platform is not without challenges, though, which include hour-scale response times for transcriptional regulation based sensors, long times to return to baseline, and the requirement for adequate growth nutrients in the environment [8, 9]. These drawbacks will limit the deployment of whole-cell electrochemical biosensing technology, but improvements can also be made by focusing on allosteric response pathways [44] or integrating nutrient reservoirs into the device [45].

Applications for this biosensing platform extend far beyond fumarate and are only limited by the chemicals we can genetically engineer electrogenic bacteria to be sensitive to. With development in arsenic [24] and arabinose [25] sensing *S. oneidensis*, as well as introduction of the exoelectrogenic MR-1 Mtr pathway to *E. coli* [23, 46, 47], there are numerous opportunities to sense a variety of vital chemicals by engineering the outer membrane protein

complexes. Further work could be pursued through additional miniaturization and reduction of power of (1) the abiotic core through ASIC design, and (2) the biotic component by customization of reference electrode and using a smaller volume reactor. The ability to interface low power electronics with robust, sensing, exoelectrogenic bacteria such as *S. oneidensis* shows potential in efforts towards continuous, real-time monitoring of aquatic environments.

Bibliography

- [1] E. J. Chua, W. Savidge, R. T. Short, A. M. Cardenas-Valencia, and R. W. Fulweiler, “A Review of the Emerging Field of Underwater Mass Spectrometry,” *Frontiers in Marine Science*, vol. 3, pp. 1–24, nov 2016.
- [2] C. I. L. Justino, A. C. Freitas, A. C. Duarte, and T. A. P. R. Santos, “Sensors and biosensors for monitoring marine contaminants,” *Trends in Environmental Analytical Chemistry*, vol. 6-7, pp. 21–30, 2015.
- [3] S. Kröger and R. J. Law, “Biosensors for marine applications: We all need the sea, but does the sea need biosensors?,” in *Biosensors and Bioelectronics*, vol. 20, pp. 1903–1913, 2005.
- [4] G. Hanrahan, D. Patil, and J. Wang, “Electrochemical sensors for environmental monitoring: design, development and applications,” *Journal of environmental monitoring : JEM*, vol. 6, no. 8, pp. 657–664, 2004.
- [5] G. Mills and G. Fones, “A review of in situ methods and sensors for monitoring the marine environment,” *Sensor Review*, vol. 32, pp. 17–28, jan 2012.
- [6] T. S. Moore, K. M. Mullaugh, R. R. Holyoke, A. S. Madison, M. Yücel, and G. W. Luther, “Marine chemical technology and sensors for marine waters: potentials and limits.,” *Annual review of marine science*, vol. 1, pp. 91–115, jan 2009.
- [7] S. F. D’Souza, “Microbial biosensors,” 2001.
- [8] Y. Arikawa, K. Ikebukuro, and L. Karube, “Microbial Biosensors Based on Respiratory Inhibition,” in *Enzyme and Microbial Biosensors*, pp. 225–236, New Jersey: Humana Press, 1998.

- [9] A. L. Simonian, E. I. Rainina, and J. R. Wild, “Microbial biosensors based on potentiometric detection,” *Enzyme and Microbial Biosensors : Techniques and Protocols*, vol. 6, pp. 237–248, 1998.
- [10] L. Su, W. Jia, C. Hou, and Y. Lei, “Microbial biosensors: A review,” 2011.
- [11] B. E. Logan, “Exoelectrogenic bacteria that power microbial fuel cells,” *Nature Reviews Microbiology*, vol. 7, pp. 375–381, may 2009.
- [12] H. Wang and Z. J. Ren, “A comprehensive review of microbial electrochemical systems as a platform technology,” 2013.
- [13] D. Grieshaber, R. Mackenzie, J. Vörös, and E. Reimhult, “Electrochemical Biosensors -Sensor Principles and Architectures,” *Sensors*, vol. 8, no. 3, pp. 1400–1458, 2008.
- [14] P. W. Rundel, E. A. Graham, M. F. Allen, J. C. Fisher, and T. C. Harmon, “Environmental sensor networks in ecological research,” may 2009.
- [15] X. Yang, K. G. Ong, W. R. Dreschel, K. Zeng, C. S. Mungle, and C. A. Grimes, “Design of a Wireless Sensor Network for Long-term, In-Situ Monitoring of an Aqueous Environment,” *Sensors*, vol. 2, pp. 455–472, nov 2002.
- [16] D. Pant, G. Van Bogaert, L. Diels, and K. Vanbroekhoven, “A review of the substrates used in microbial fuel cells (MFCs) for sustainable energy production,” 2010.
- [17] O. Bretschger, A. Obraztsova, C. A. Sturm, S. C. In, Y. A. Gorby, S. B. Reed, D. E. Culley, C. L. Reardon, S. Barua, M. F. Romine, J. Zhou, A. S. Beliaev, R. Bouhenni, D. Saffarini, F. Mansfeld, B. H. Kim, J. K. Fredrickson, and K. H. Nealson, “Current production and metal oxide reduction by *Shewanella oneidensis* MR-1 wild type and mutants,” *Applied and Environmental Microbiology*, vol. 73, pp. 7003–7012, nov 2007.
- [18] A. Y. Zhou, T. J. Zajdel, M. A. Teravest, and M. M. Maharbiz, “A miniaturized monitoring system for electrochemical biosensing using *Shewanella oneidensis* in environmental applications,” in *Proceedings of the Annual International Conference of the IEEE Engineering in Medicine and Biology Society, EMBS*, vol. 2015-Novem, pp. 7518–7521, IEEE, aug 2015.

- [19] D. Coursolle, D. B. Baron, D. R. Bond, and J. A. Gralnick, “The Mtr respiratory pathway is essential for reducing flavins and electrodes in *Shewanella oneidensis*,” *Journal of Bacteriology*, vol. 192, pp. 467–474, jan 2010.
- [20] K. Rabaey and R. A. Rozendal, “Microbial electrosynthesis - revisiting the electrical route for microbial production.,” *Nature reviews. Microbiology*, vol. 8, pp. 706–16, oct 2010.
- [21] L. M. Tender, S. A. Gray, E. Groveman, D. A. Lowy, P. Kauffman, J. Melhado, R. C. Tyce, D. Flynn, R. Petrecca, and J. Dobarro, “The first demonstration of a microbial fuel cell as a viable power supply: Powering a meteorological buoy,” *Journal of Power Sources*, vol. 179, no. 2, pp. 571–575, 2008.
- [22] Z. Li, M. A. Rosenbaum, A. Venkataraman, T. K. Tam, E. Katz, and L. T. Angenent, “Bacteria-based AND logic gate: a decision-making and self-powered biosensor,” *Chemical Communications*, vol. 47, no. 11, p. 3060, 2011.
- [23] M. A. Teravest, T. J. Zajdel, and C. M. Ajo-Franklin, “The Mtr Pathway of *Shewanella oneidensis* MR-1 Couples Substrate Utilization to Current Production in *Escherichia coli*,” *ChemElectroChem*, vol. 1, pp. 1874–1879, nov 2014.
- [24] D. P. Webster, M. A. TerAvest, D. F. R. Doud, A. Chakravorty, E. C. Holmes, C. M. Radens, S. Sureka, J. A. Gralnick, and L. T. Angenent, “An arsenic-specific biosensor with genetically engineered *Shewanella oneidensis* in a bioelectrochemical system,” *Biosensors and Bioelectronics*, vol. 62, pp. 320–324, 2014.
- [25] F. Golitsch, C. Bücking, and J. Gescher, “Proof of principle for an engineered microbial biosensor based on *Shewanella oneidensis* outer membrane protein complexes,” *Biosensors and Bioelectronics*, vol. 47, pp. 285–291, 2013.
- [26] E. S. Friedman, M. A. Rosenbaum, A. W. Lee, D. A. Lipson, B. R. Land, and L. T. Angenent, “A cost-effective and field-ready potentiostat that poises subsurface electrodes to monitor bacterial respiration,” *Biosensors and Bioelectronics*, vol. 32, no. 1, pp. 309–313, 2012.
- [27] Y. Lei, W. Chen, and A. Mulchandani, “Microbial biosensors,” 2006.

- [28] H. J. Shin, “Genetically engineered microbial biosensors for in situ monitoring of environmental pollution,” *Applied Microbiology and Biotechnology*, vol. 89, pp. 867–877, feb 2011.
- [29] F. Harnisch and S. Freguia, “A basic tutorial on cyclic voltammetry for the investigation of electroactive microbial biofilms,” mar 2012.
- [30] C. R. Myers and K. H. Nealson, “Bacterial manganese reduction and growth with manganese oxide as the sole electron acceptor.,” *Science*, vol. 240, no. 4857, pp. 1319–1321, 1988.
- [31] D. Coursolle and J. A. Gralnick, “Reconstruction of extracellular respiratory pathways for iron(III) reduction in *Shewanella oneidensis* strain MR-1,” *Frontiers in Microbiology*, vol. 3, no. FEB, p. 56, 2012.
- [32] D. E. Ross, J. M. Flynn, D. B. Baron, J. A. Gralnick, and D. R. Bond, “Towards electrosynthesis in *Shewanella*: Energetics of reversing the Mtr pathway for reductive metabolism,” *PLoS ONE*, vol. 6, p. e16649, feb 2011.
- [33] S. Stretton, S. Techkarnjanaruk, A. M. McLennan, and A. E. Goodman, “Use of green fluorescent protein to tag and investigate gene expression in marine bacteria.,” *Applied and environmental microbiology*, vol. 64, pp. 2554–2559, jul 1998.
- [34] Y. A. Gorby, S. Yanina, J. S. McLean, K. M. Rosso, D. Moyles, A. Dohnalkova, T. J. Beveridge, I. S. Chang, B. H. Kim, K. S. Kim, D. E. Culley, S. B. Reed, M. F. Romine, D. A. Saffarini, E. A. Hill, L. Shi, D. A. Elias, D. W. Kennedy, G. Pinchuk, K. Watanabe, S. Ishii, B. Logan, K. H. Nealson, and J. K. Fredrickson, “Electrically conductive bacterial nanowires produced by *Shewanella oneidensis* strain MR-1 and other microorganisms.,” *Proceedings of the National Academy of Sciences of the United States of America*, vol. 103, pp. 11358–63, jul 2006.
- [35] S. Pirbadian, S. E. Barchinger, K. M. Leung, H. S. Byun, Y. Jangir, R. A. Bouhenni, S. B. Reed, M. F. Romine, D. A. Saffarini, L. Shi, Y. A. Gorby, J. H. Golbeck, and M. Y. El-Naggar, “*Shewanella oneidensis* MR-1 nanowires are outer membrane and periplasmic extensions of the extracellular electron transport components.,” *Proceedings of the*

National Academy of Sciences of the United States of America, vol. 111, pp. 12883–8, sep 2014.

- [36] K. Venkateswaran, D. P. Moser, M. E. Dollhopf, D. P. Lies, D. A. Saffarini, B. J. MacGregor, D. B. Ringelberg, D. C. White, M. Nishijima, H. Sano, J. Burghardt, E. Stackebrandt, and K. H. Nealson, “Polyphasic taxonomy of the genus *Shewanella* and description of *Shewanella oneidensis* sp. nov.,” *International journal of systematic bacteriology*, vol. 49 Pt 2, pp. 705–24, apr 1999.
- [37] B. Fonseca, C. Paquete, S. Neto, I. Pacheco, C. Soares, and R. Louro, “Mind the gap: cytochrome interactions reveal electron pathways across the periplasm of *Shewanella oneidensis* MR-1,” *Biochemical Journal*, vol. 108, no. 1, pp. 101–108, 2013.
- [38] B. Schuetz, M. Schicklberger, J. Kuermann, A. M. Spormann, and J. Gescher, “Periplasmic electron transfer via the c-type cytochromes Mtra and Fcca of *Shewanella oneidensis* Mr-1,” *Applied and Environmental Microbiology*, vol. 75, pp. 7789–7796, dec 2009.
- [39] T. E. Meyer, A. I. Tsapin, I. Vandenberghe, L. de Smet, D. Frishman, K. H. Nealson, M. A. Cusanovich, and J. J. van Beeumen, “Identification of 42 possible cytochrome C genes in the *Shewanella oneidensis* genome and characterization of six soluble cytochromes,” *Omics : a journal of integrative biology*, vol. 8, pp. 57–77, jan 2004.
- [40] M. Di Lorenzo, T. P. Curtis, I. M. Head, and K. Scott, “A single-chamber microbial fuel cell as a biosensor for wastewaters,” *Water Research*, vol. 43, no. 13, pp. 3145–3154, 2009.
- [41] Y. Zhang and I. Angelidaki, “A simple and rapid method for monitoring dissolved oxygen in water with a submersible microbial fuel cell (SBMFC),” *Biosensors and Bioelectronics*, vol. 38, no. 1, pp. 189–194, 2012.
- [42] L. Peixoto, B. Min, G. Martins, A. G. Brito, P. Kroff, P. Parpot, I. Angelidaki, and R. Nogueira, “In situ microbial fuel cell-based biosensor for organic carbon,” *Bioelectrochemistry*, vol. 81, no. 2, pp. 99–103, 2011.
- [43] Y. Zhang and I. Angelidaki, “Submersible microbial fuel cell sensor for monitoring microbial activity and BOD in groundwater: Focusing on impact of anodic biofilm on

sensor applicability,” *Biotechnology and Bioengineering*, vol. 108, pp. 2339–2347, oct 2011.

- [44] F. Zhang and J. Keasling, “Biosensors and their applications in microbial metabolic engineering,” 2011.
- [45] L. H. Larsen, T. Kjær, and N. P. Revsbech, “A microscale NO₃- biosensor for environmental applications,” *Biosensors and Bioelectronics*, vol. 69, pp. 3527–3531, 1997.
- [46] C. P. Goldbeck, H. M. Jensen, M. A. Teravest, N. Beedle, Y. Appling, M. Hepler, G. Cambray, V. Mutalik, L. T. Angenent, and C. M. Ajo-Franklin, “Tuning promoter strengths for improved synthesis and function of electron conduits in *Escherichia coli*,” *ACS Synthetic Biology*, vol. 2, pp. 150–159, mar 2013.
- [47] H. M. Jensen, A. E. Albers, K. R. Malley, Y. Y. Londer, B. E. Cohen, B. A. Helms, P. Weigele, J. T. Groves, and C. M. Ajo-Franklin, “Engineering of a synthetic electron conduit in living cells,” *Proc Natl Acad Sci U S A*, vol. 107, pp. 19213–19218, nov 2010.

Appendices

Version 1 of BESSY

The first version of BESSY performed one-channel potentiometric analysis and did not have wireless communication capabilities, rendering a user unknowledgable in real time. Specifically, a COTS microcontroller (MSP430FG43x) with integrated DACs, ADCs, and op amps was programmed to reproduce the functions of a potentiostat. The on-chip DAC was used to output a 200 mV potential which was summed with the Ag/AgCl RE so that the potential of the cells on the WE was 200 mV above the reference. The electrochemical current was dropped across a load ($R_2=270 \Omega$) and that voltage was amplified and converted back to current using the onchip ADC and μP (Fig. 11a). Due to the limited storage capability of the microcontroller, the data was logged through UART to OpenLog, available on Sparkfun. This allowed us to see current trends over long periods of time, but only upon termination of the experiment, when the SD card was removed and data analyzed. The complete electronics package is shown in Figure 11b. The total footprint of the COTS components is 18X20 mm and the data logger is 15X19 mm, with a combined width of 8mm.

In order to ensure that the electrochemical signal is due only to the encapsulated *S. oneidensis*, and not an environmental contaminant, we package the sensing device in a PDMS casing cast from a 3D-printed ABS mold. This cylindrical raft (25 mm radius, 80 mm height) encloses the three electrodes and a 50 mL suspended solution of *S. oneidensis* in M1 medium (Fig. 11c). The WE is comprised of carbon felt with a 2400 mm² surface area, the RE is a standard, commercially available Ag/AgCl reference (CHI111 from CH Instruments, Inc.), and the CE is a platinum wire. This wet portion of the cell is protected from the environment by a 0.2 μm PTFE filter of 47 mm diameter, attached to the PDMS with silicone rubber. The raft also includes a cutout which is not exposed to solutions and will house the electronic components. This creates a free-floating, fully encapsulated, miniaturized package that requires only power inputs during run time.

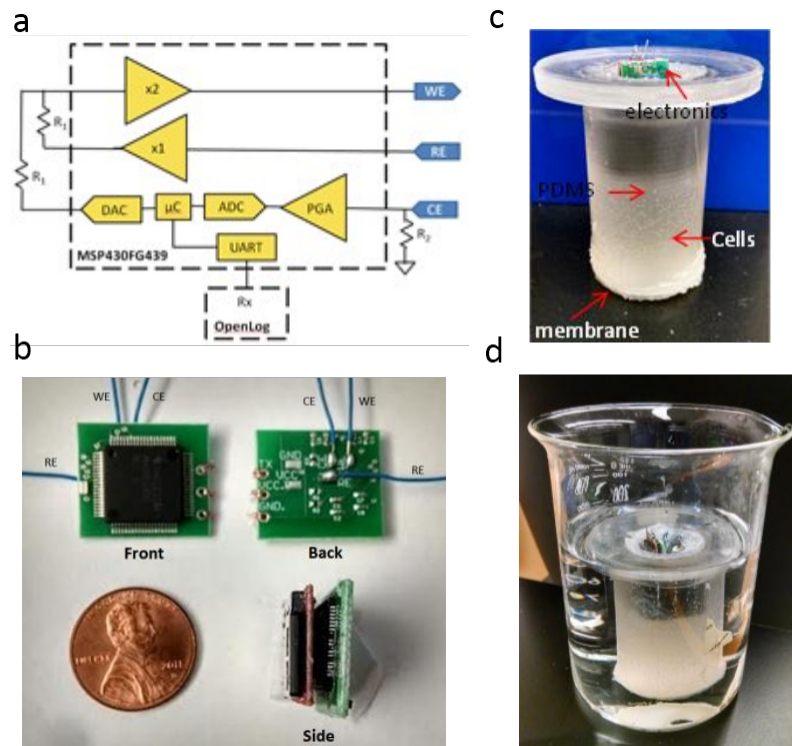


Figure 11: **Version 1 of BESSY** (a) Circuit diagram of the components of the COTS miniaturized potentiostat. R_1 is chosen to be $1\text{ k}\Omega$ and R_2 is $270\ \Omega$. Programmable gain amplifier varies from $1\times$ to $16\times$ gain and determines resolution of the potentiostat with the 12-bit ADC. The DAC outputs 0 to 1V to set the WE to a specified potential higher than the RE. (b) 18×20 mm printed circuit board potentiostat (green) attached to the OpenLog data logger with microSD card (red), making the total thickness 8mm. Front side includes MCU and 32 kHz crystal, back side includes discrete components for amplifiers and power stability in addition to pads to WE, RE, and CE (three blue wires). The only input required at runtime in this iteration of the chip is power and ground. (c) PDMS packaging encapsulating the electronics, electrodes, and *S. oneidensis* sensor cells. (d) Packaged sensor floating in a 1 L beaker of M1 medium containing 50mM pyruvate.

A step-by-step guide to constructing an m-reactor

Reminder: Assembly of m-reactor should take place in a sterile environment; we recommend a sterile biohood. The following procedure details the steps to create a $2 \times 1 \times 1 \text{ cm}^3$ m-reactor.

B.1 Preparation

- 3D print scaffolds using PLA (one per m-reactor)

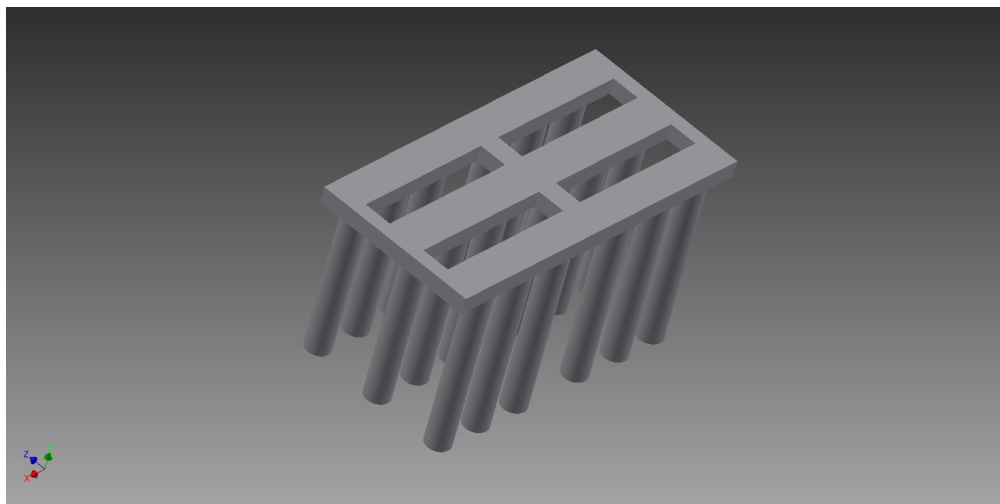


Figure 12: **Scaffold** Structure consists of checkered base with 18 cylindrical pillars emerging. Base dimension measures $2 \times 1 \times 0.1 \text{ cm}^3$ with four $0.85 \times 0.17 \times 0.1 \text{ cm}^3$ holes cut out. The pillars are 0.15 cm diameter and 0.9 cm tall.

- Grow bacteria overnight in nutrient rich broth until $OD_{600nm} \approx 120$. Prepare at least 150 μL of suspension per m-reactor. (See specific strain information sheets for optimal growth conditions)
- Sterilize all tools with 70% ethanol unless otherwise stated:
 1. Titanium wire (2 per m-reactor)
 2. M-reactor mold
 3. Shredded carbon felt (250 mg per m-reactor) by UV sterilizing for 10 minutes
 4. Exacto knife
 5. Scaffolds (3D printed PLA)
 6. Compression tool (ex. metal spatula)
- Wrap titanium wire around top bridge of scaffold, allow at least 4 cm sticking out.
- Prepare 1% agarose and store in 55°C water bath (~ 5 mL per m-reactor)
- Prepare 0.5% agarose and store in 55°C wafer bath (enough to submerge m-reactor completely for coating)

B.2 Construction

1. Add 150 μL of cell suspension to 250 mg carbon felt and mix well, until all carbon felt is wet
2. Add 1.4 mL of 1% agarose to felt and mix well
3. Coat mold with 1% agarose
4. Add agarose-felt mixture into mold and compress
5. Insert scaffold to compressed agarose-felt mixture
6. Add 1% agarose to cover scaffold
7. Let solidify and cool down for at least 15 minutes at room temperature

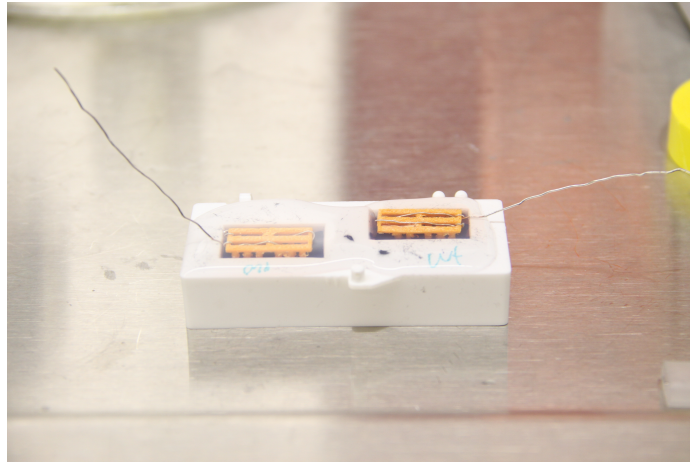


Figure 13: Reactors cooling down for agarose solidification at room temperature within the reactor molds.

8. Extract the reactors from the mold using the exacto knife to carefully release the structure

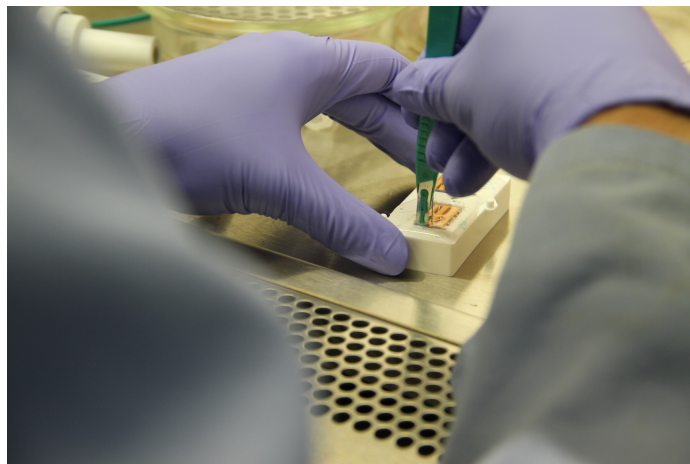


Figure 14: Carefully extracting the reactors from the mold by releasing the agarose using a sterilized exacto knife

9. Insert second titanium wire to carbon felt portion of the reactor
10. Dip structure into beaker of 0.5% agarose
11. Place in dessicator with 8 mL of tetramethyl orthosilicate (TMOS) for ~2 hours.

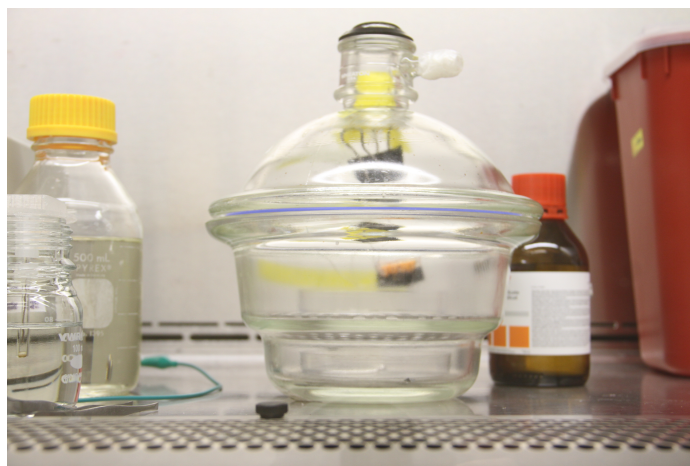


Figure 15: Reactors shown in dessicator for silica deposition

12. Remove from dessicator. This is completed m-reactor!

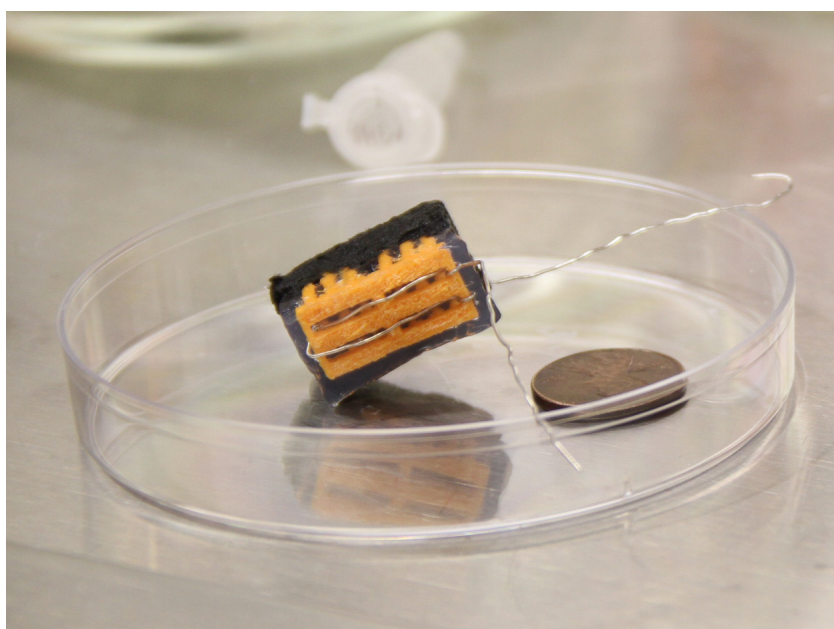


Figure 16: Final m-reactor

B.3 After-care

Tips for storing m-reactors:

- Place into aqueous environment as soon as possible to prevent agarose from drying out. We recommend submersing in medium similar to environment in which you will run sensing experiments from (in this case, M9 medium).
- Place tubes with reactors and medium on ice if not using immediately.
- Try to minimize disruption of the silica filter layer to prevent contamination of exoelectrogenic bacteria.

Potentiostat Code

C.1 MSP430 C Code

This code was compiled using Code Composer and flashed to the MSP430 microprocessor through an MSP430 USB-Debug-Interface (MSP-FET430UIF) to a 80-pin Target Development Board (MSP-RS430PN80) containing the MSP430FG43x.

```
#include <msp430.h>
#include <stdio.h>
#include <stdarg.h>

#define totalTime      2880           //in minutes
#define interval      15             //in seconds
#define potVoltage     200           //in mV
#define resistor       1000          //in ohms
#define startRes       4             //gain = [1,1.3,2,2.7,4,5.3,8,16]

static int numData = 11521;          //number of data points
static unsigned int ADCresult, gain = startRes;
float current;                       //in uA
long time, longc;                    //in minutes and nA
unsigned long seconds, count, start; //time in seconds, counter for TA
float currentMax, currentMaxPlus, dividend, currentNow;
char outputstr[35];                  //string to UART
int i, volt, testNum, channelCounter, channelFlag;

void readADC(int num){               //read value at ADC and calibrate to current
    double inCurrent;
```

```

ADC12CTL0 |= ADC12SC;          // Start conversion
while ((ADC12IFG & BIT0)==0);
ADCResult = ADC12MEM0;
inCurrent = ((double)ADCResult)/dividend;
current = inCurrent;
currentNow = inCurrent;
}

void setVoltage(double voltage){ //set output of DAC to voltage (in mV)
    int dacValue;
    dacValue = voltage*4.096/1.5;
    DAC121DAT = dacValue;
}

void runTest(double v, unsigned int test){
    volatile unsigned int i;
    time = seconds-start;
    readADC(test);
}

void changeResolution(int g){
    static float gainVal[8]={1, 1.3, 2, 2.7, 4, 5.3, 8, 16};
    if (g==0){
        OA0CTL1 = OAFB0_0 + OARRIP + OAFBR_0;    //1x gain
    }
    else if (g==1){
        OA0CTL1 = OAFB0_1 + OARRIP + OAFBR_1;    //1.3x gain
    }
    else if (g==2){
        OA0CTL1 = OAFB0_2 + OARRIP + OAFBR_2;    //2x gain
    }
    else if (g==3){
        OA0CTL1 = OAFB0_3 + OARRIP + OAFBR_3;    //2.7x gain
    }
    else if (g==4){
        OA0CTL1 = OAFB0_4 + OARRIP + OAFBR_4;    //4x gain
    }
    else if (g==5){
        OA0CTL1 = OAFB0_5 + OARRIP + OAFBR_5;    //5.3x gain
    }
}

```

```

}
else if (g==6){
    OA0CTL1 = OAFB_4 + OARRIP + OAFBR_6;    //8x gain
}
else if (g==7){
    OA0CTL1 = OAFB_4 + OARRIP + OAFBR_7;    //16x gain
}
else {
    OA0CTL1 = OAFB_4 + OARRIP + OAFBR_4;    //4x gain default
}
dividend = .00273*gainVal[g]*resistor;
currentMax = 1500000/gainVal[g]/resistor;
if(g!=7){
    currentMaxPlus = 1500000/gainVal[g+1]/resistor;
}
}

int main(void)
{
    WDICIL = WDIPW + WDIHOLD;                // Stop watchdog timer
    FLL_CTL0 |= XCAP18PF;                    // Set load capacitance for xtal

    //DMA to UART setup
    P2SEL = 0x10;                            // P2.4 = USART0 TXD
    ME1 |= UTXE0;                            // Enabled USART0 TXD
    UCTL0 |= CHAR;                          // 8-bit character, SWRST=1
    UTCTL0 |= SSEL1;                        // UCLK = SMCLK
    UBR00 = 0x36;                          // 19200 from ~1Mhz
    UBR10 = 0x00;
    UMCTL0 = 0x6B;                          // Modulation
    UCTL0 &= ~SWRST;                        // Initialize USART state machine
    DMA0SA = (int)outputstr;                // Source string address
    DMA0DA = (unsigned int)&U0TXBUF;       // Destination single address
    DMACTL0 = DMA0TSEL_2;                   // TBCCR2 trigger
    TBCTL = TBSSEL_2 + ID_2 + MC_2;        // setup timer B: SMCLK/4

    //ADC setup
    P5SEL |= 0x01;                          // Enable A/D channel A13
    ADC12CTL0 = ADC12ON+SHT0_2+REFON;      // Turn on ADC12, set sampling time

```

```

ADC12CTL1 = SHP; // Use sampling timer
ADC12MCTL0 = SREF_1+INCH_13; // Input channel A13
for (i=0; i<0x3600; i++){ // Delay for reference start-up
ADC12CTL0 |= ENC; // Enable conversions
testNum=0;

//DAC setup
DAC12_1CTL = DAC12IR + DAC12AMP_2 + DAC12ENC + DAC12CALON;

//OA0 to noninverting pga mode with gain = 4
OA0CTL0 = OAPM1 + OAADC1; // Select inputs, power mode
changeResolution(startRes); // Mode, OAFBRx sets gain

//OA1 to noninverting pga mode with gain = 2
OA1CTL0 = OAPM1 + OAADC1; // Select inputs, power mode
OA1CTL1 = OAF_4 + OAFBR_2 + OARRIP; // Mode, OAFBRx sets gain (G=2)

//OA2 to unity gain voltage buffer mode
OA2CTL0 = OAPM1 + OAADC1; // Select inputs, power mode
OA2CTL1 = OAF_4 + OAFBR_0 + OARRIP; // Mode, rail-to-rail inputs

//timer A setup
seconds = 0; count = 0;
P5DIR |= 0x02; // P5.1 output
TACCTL0 = CCIE; // CCR0 interrupt enabled
TACCR0 = 61440;
TACTL = TASSEL_1 + MC_2 + ID_3; // ACLK, continuous mode
P4DIR |= 0x02;
P4OUT = 0x00;

//write header
__delay_cycles(2000000); // Initialize redbear or openlog
__bis_SR_register(GIE); // Enter LPM0

//initialize variables
setVoltage(200);
start = seconds;
count = start+15;
volt = potVoltage;

```

```

channelCounter = 0;
channelFlag = 1;

while(1){

// Timer A0 interrupt service routine
#if defined(__TI_COMPILER_VERSION__) || defined(__IAR_SYSTEMS_ICC__)
#pragma vector=TIMER_A0_VECTOR
__interrupt void Timer_A (void)
#elif defined(__GNUC__)
void __attribute__((interrupt(TIMER_A0_VECTOR))) Timer_A (void)
#else
#error Compiler not supported!
#endif
{
    P5OUT ^= 0x02;           // Toggle P5.1 for debugging
    seconds+=15;
    CCR0 += 61440;          // Add Offset to CCR0

    channelCounter += 1;

    //read and convert ADC
    runTest(volt , testNum++);

    //output to UART
    longc = (long)(current*1000);
    sprintf (outputstr , "%ld,%ld,%d_\r\n", time , longc , channelFlag);
    DMA0SA = (int)outputstr; // Source string address
    DMA0SZ = strlen(outputstr);
    DMA0CTL = DMADT.1 + DMASRCINCR.3 + DMALEVEL + DMASBDB + DMAEN;

    if(channelCounter > 39){
        channelCounter = 0;
        P4OUT ^= 0x02;
        if(channelFlag == 1){
            channelFlag = 2;
        }
        else {
            channelFlag = 1;

```

```

    }
}

//check resolution and autoadjust if necessary
if((ADCresult > 3995 )&&(gain!=0)){
    gain--;
    changeResolution(gain);
}
if((ADCresult < 100 )&&(gain!=7)){
    gain++;
    changeResolution(gain);
}
}
}

```

C.2 RedBear Labs Energia Code

Note: Skeleton for this code is sample code available through Energia[©]Temboo, Inc. Example Code: "Send data to google spreadsheet." Personal contribution in void loop: read from port 1, send to port 0.

```

/*****
Demonstrates how to update a Google Spreadsheet from your
TI LaunchPad using Temboo and the Google Spreadsheets API.

Learn to auto-generate your own code for the TI LaunchPad
with Temboo's Getting Started examples and tutorials.

** http://temboo.com/hardware/ti **

*****/

/*
Instructions:

1. Create a Temboo account: http://www.temboo.com

2. Retrieve your Temboo application details: http://www.temboo.com/account/

```

↪ *applications*

3. *Replace the values in the TembooAccount.h tab with your Temboo*

↪ *application details*

4. *You'll also need a Google Spreadsheet that includes a title in the first*

↪ *row*

of each column that data will be written to. This example saves values to

↪ *three columns:*

company, location, and contact. The spreadsheet should be set up with

↪ *three column names:*

| <i>Company</i> | <i>Location</i> | <i>Contact</i> |
|----------------|-----------------|----------------|
| | | |

5. *Google Spreadsheets requires you to authenticate via OAuth. Follow the*

↪ *steps in the link below to find your ClientID, ClientSecret, and*

↪ *RefreshToken, and then use those values to overwrite the placeholders*

↪ *in the code below.*

<https://temboo.com/library/Library/Google/OAuth/>

For the scope field, you need to use:

<https://spreadsheets.google.com/feeds/>

Here's a video outlines how Temboo helps with the OAuth process:

<https://www.temboo.com/videos#oauthchoreos>

And here's a more in-depth version of this example on our website:

<https://temboo.com/hardware/ti/update-google-spreadsheet>

6. *Next, upload the sketch to your LaunchPad and open Energia's serial*

↪ *monitor*

Note: you can test this Choreo and find the latest instructions on our

↪ *website: <https://temboo.com/library/Library/Google/Spreadsheets/>*

↪ *AppendRow/*

This example code is in the public domain.


```

*/

#include <SPI.h>
#include <WiFi.h>
#include <WiFiClient.h>
#include <Temboo.h>
#include "TembooAccount.h" // contains Temboo account information
                          // as described in the footer comment below

/** SUBSTITUTE YOUR VALUES BELOW: */

// note that for additional security and reusability, you could
// use #define statements to specify these values in a .h file.

// the clientID found in Google's Developer Console under APIs & Auth >
  ↪ Credentials
const String CLIENT_ID = "your-client-id";

// the clientSecret found in Google's Developer Console under APIs & Auth >
  ↪ Credentials
const String CLIENT_SECRET = "your-client-secret";

// returned after running FinalizeOAuth
const String REFRESH_TOKEN = "your-oauth-refresh-token";

// the name of the spreadsheet in your Google Docs/Drive
// that you want to send data to
const String SPREADSHEET_TITLE = "your-spreadsheet-title";

// the data you'd like to add to your spreadsheet, each cell value separated
  ↪ by a comma
const String ROWDATA = "Temboo, _New_York, _hey@temboo.com";

WiFiClient client;

void setup() {
  Serial.begin(9600);
  Serial1.begin(19200);

```

```

int wifiStatus = WL_IDLE_STATUS;

// determine if the WiFi Shield is present.
Serial.print("\n\nShield:");
if (WiFi.status() == WL_NO_SHIELD) {
    Serial.println("FAIL");
    // if there's no WiFi shield, stop here.
    while(true);
}

while(wifiStatus != WL_CONNECTED) {
    Serial.print("WiFi:");
    wifiStatus = WiFi.begin(WIFI_SSID); //, WIFIPASSWORD);
    if (wifiStatus == WL_CONNECTED) {
        Serial.println("OK");
    } else {
        Serial.println("FAIL");
    }
    delay(5000);
}

void loop() {

    char inByte;

    // read from port 1, send to port 0:
    if (Serial1.available()) {
        inByte = Serial1.read();
        stringOut += inByte;
        Serial.write(inByte);

        if(inByte=='\n'){

            Serial.println(stringOut);
            Serial.println("Appending_value_to_spreadsheet...");

            // we need a Process object to send a Choreo request to Temboo
            TembooChoreo AppendRowChoreo(client);

```

```

// invoke the Temboo client
// NOTE that the client must be reinvoked and repopulated with
// appropriate arguments each time its run() method is called.
AppendRowChoreo.begin();

// set Temboo account credentials
AppendRowChoreo.setAccountName(TEMBOO_ACCOUNT);
AppendRowChoreo.setAppKeyName(TEMBOO_APP_KEY_NAME);
AppendRowChoreo.setAppKey(TEMBOO_APP_KEY);

// identify the Temboo Library choreo to run (Google > Spreadsheets >
  ↪ AppendRow)
AppendRowChoreo.setChoreo("/Library/Google/Spreadsheets/AppendRow");

// your Google application client ID
AppendRowChoreo.addInput("ClientID", CLIENT_ID);
// your Google application client secret
AppendRowChoreo.addInput("ClientSecret", CLIENT_SECRET);
// your Google OAuth refresh token
AppendRowChoreo.addInput("RefreshToken", REFRESH_TOKEN);
// the data you want to append to the spreadsheet
AppendRowChoreo.addInput("RowData", stringOut);
// the title of the spreadsheet you want to append to
AppendRowChoreo.addInput("SpreadsheetTitle", SPREADSHEET_TITLE);

// run the Choreo and wait for the results
// the return code (returnCode) will indicate success or failure
unsigned int returnCode = AppendRowChoreo.run();

// a return code of zero (0) means everything worked
if (returnCode == 0) {
    Serial.println("Success!_Spreadsheet_updated!\n");
}
else {
    // a non-zero return code means there was an error
    // read and print the error message
    while (AppendRowChoreo.available()) {
        char c = AppendRowChoreo.read();
    }
}

```

```

        Serial.print(c);
    }
}

AppendRowChoreo.close();
stringOut = "";
}
}
}

/*
IMPORTANT NOTE: TembooAccount.h:

TembooAccount.h is a file referenced by this sketch that contains your
↳ Temboo account information. You'll need to edit the placeholder
↳ version of TembooAccount.h included with this example sketch, by
↳ inserting your own Temboo account name and app key information. The
↳ contents of the file should look like:

#define TEMBOO_ACCOUNT "myTembooAccountName" // your Temboo account name
#define TEMBOO_APP_KEY_NAME "myFirstApp" // your Temboo app name
#define TEMBOO_APP_KEY "xxxxxxxxxxxxxx" // your Temboo app key

#define WIFLSSID "myWiFiNetworkName"
#define WIFLPASSWORD "myWiFiNetworkPassword"

You can find your Temboo App Key information on the Temboo website under
↳ Account > Applications

The same TembooAccount.h file settings can be used for all Temboo sketches.

Keeping your account information in a separate file means you can share the
↳ main sketch file without worrying that you forgot to delete your
↳ credentials.
*/

```

C.3 Matlab Code for Extracting Steady State Current

This matlab code parses an imported spreadsheet of time and current data from the BESSY and both separates the single column of data into two distinct channels, and finds the steady state current value of the m-reactor at each 10 minute interval.

```
%% import data
datain = importdata('C:\datafile.csv');

datasize = size(datain.data);
datasets = datasize(2)-1;

time = datain.data(:,1);
current = datain.data(:,2:datasets+1);

%% initialize variables
vo_ch1_2 = zeros(floor(length(current)/80), datasets);
vo_ch2_2 = zeros(floor(length(current)/80), datasets);
tau_ch1_2 = zeros(floor(length(current)/80), datasets);
tau_ch2_2 = zeros(floor(length(current)/80), datasets);
i_ch1_2 = zeros(floor(length(current)/80), datasets);
i_ch2_2 = zeros(floor(length(current)/80), datasets);

%% fit to exponential decay curve
options = fitoptions('exp2','Lower',[-inf -inf -inf 0], 'Upper', [inf inf inf
    ↪ 0]);

for k = 1:datasets

    for i = 1:floor(length(current(:,k))/40);
        x = time(((i-1)*40+1):((i-1)*40+40));
        y = current(((i-1)*40+1):((i-1)*40+40),k);
        try
            f=fit(x,y,'exp2',options);
        catch ME
            disp('No_conversion_for_data_k,i');
            disp(k); disp(i);
        continue
    end
end
```

```

end

coeff = coeffvalues(f);

if mod(i,2) == 1;
    vo_ch1_2(floor(i/2)+1,k) = coeff(1);
    tau_ch1_2(floor(i/2)+1,k) = coeff(2);
    i_ch1_2(floor(i/2)+1,k) = coeff(3);
else
    vo_ch2_2(i/2,k) = coeff(1);
    tau_ch2_2(i/2,k) = coeff(2);
    i_ch2_2(i/2,k) = coeff(3);
end

end

end

%% plot for raw data, zoomed raw data, and resulting curves

subplot(2,2,1)
plot(time,current(:,1))
axis([0 150000 0 40])
xlabel('time(s)')
ylabel('current(uA)')
title('raw_data_(partial)')

subplot(2,2,2)
plot(time,current(:,1))
axis([105000 120000 0 40])
xlabel('time(s)')
ylabel('current(uA)')
title('zoomed_in_raw_data')

subplot(2,2,3)
hold on
plot(t,i_ch1(:,1),t,i_ch1(:,2),t,i_ch1(:,3));
plot(t,i_ch2(:,1),t,i_ch2(:,2),t,i_ch2(:,3));
xlabel('time(s)')

```

```

ylabel('current(uA)')
title('repeat_1_with_exponential_decay_fitting')
legend('ch1_1','ch1_2','ch1_3','ch2_1','ch2_2','ch2_3')
axis([0 170000 -2 35])

subplot(2,2,4)
hold on
plot(t2,i_ch1_2(:,1),t2,i_ch1_2(:,2),t2,i_ch1_2(:,3));
plot(t2,i_ch2_2(:,1),t2,i_ch2_2(:,2),t2,i_ch2_2(:,3));
xlabel('time(s)')
ylabel('current(uA)')
title('repeat_2_with_exponential_decay_fitting')
legend('ch1_1','ch1_2','ch1_3','ch2_1','ch2_2','ch2_3')
axis([0 170000 -2 30])

```

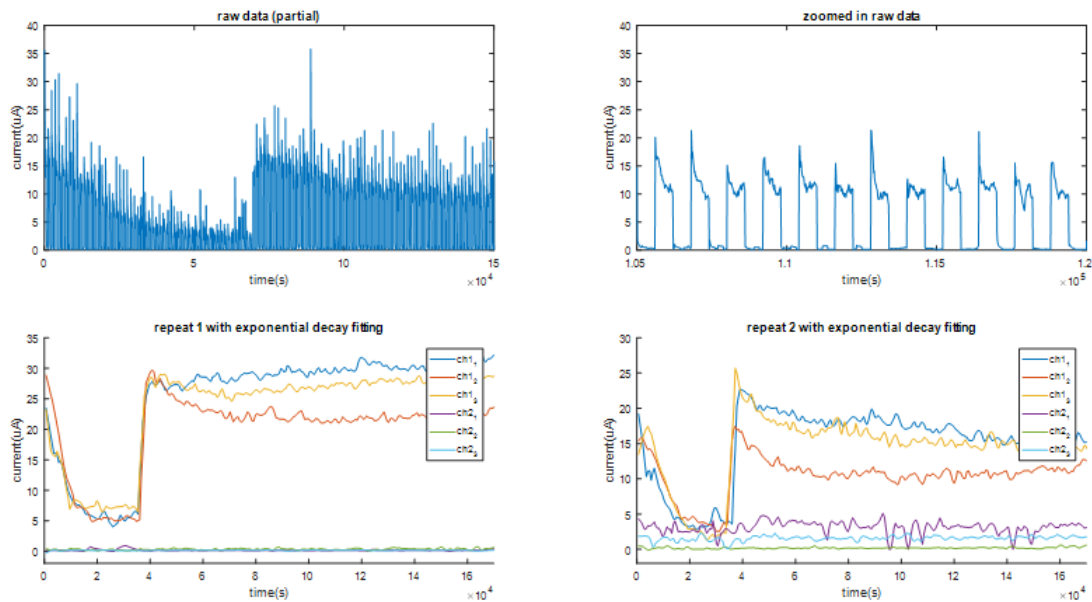


Figure 17: Sample output from matlab code. Raw data showing exponential decay across channels is split into two channels and steady state values are extrapolated for every 10 minute interval.